DOE–LM/GJ628–2004

Pinellas Environmental Restoration Project
Young-Rainey STAR Center

Reactive Transport Modeling of Enhanced Bioremediation in the Building 100 Area

April 2004

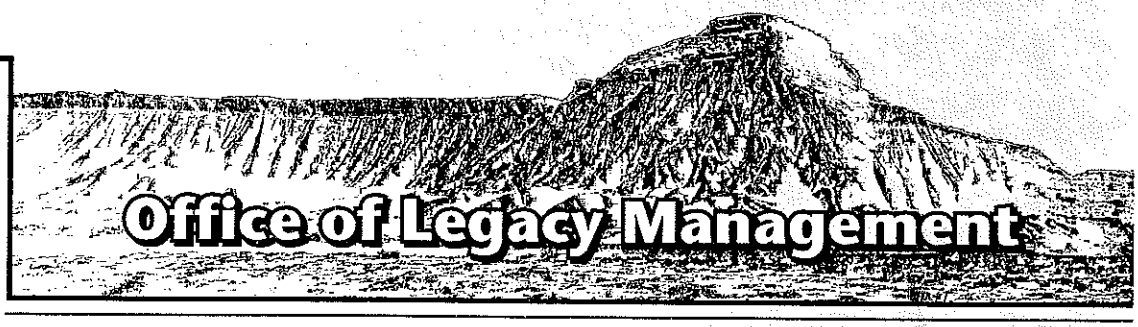

U.S. Department of Energy

Work Performed Under DOE Contract No. DE–AC01–02GJ79491
for the U.S. Department of Energy Office of Legacy Management.
Approved for public release; distribution is unlimited.

This page intentionally left blank

DOE−LM−GJ/628−2004

Pinellas Environmental Restoration Project

Young - Rainey STAR Center

Reactive Transport Modeling of Enhanced Bioremediation in the Building 100 Area

April 2004

Work Performed by S.M. Stoller Corporation under DOE Contract No. DE–AC01–02GJ79491
for the U.S. Department of Energy Office of Legacy Management, Grand Junction, Colorado

N0064700

This page intentionally left blank

Contents

1.0 Introduction 1
2.0 Background 3
2.1 Pilot Testing 3
2.2 Previous Modeling 4
2.3 Recommended Second Phase of Modeling 5
3.0 Biotransformation of Chlorinated Ethenes in Ground Water 7
3.1 General History 7
3.1.1 Natural Attenuation of Chlorinated Ethenes 7
3.1.2 Enhanced Reductive Dechlorination of Chlorinated Ethenes 10
3.1.3 Implications of Bioremediation Processes for the STAR Center 11
3.2 Monitoring Results at the Building 100 Area 12
3.2.1 Identification of Reactants 12
3.2.2 Observed Trends 13
4.0 Modeling Approach 17
4.1 BIOMOC Code 17
4.2 Governing Equations 18
4.3 Biodegradation Kinetics 20
5.0 Model Development and Findings 23
5.1 Ground Water Flow 24
5.2 Advective-Dispersive Transport 24
5.3 Biologically-Mediated Reactions 25
5.4 Simulated Bacterial Populations 28
5.5 Model Testing and Calibration 29
5.5.1 Model Sensitivity to Parameters Affecting Ground Water Velocity 29
5.5.2 Effects of Dispersivity 30
5.5.3 Model Sensitivity to Monod Parameters 30
5.6 Final Model Parameters 31
5.7 BIOMOC Model Results 31
5.7.1 Results During the Initial Ten Months of Testing 32
5.7.2 Estimated Concentrations One Year After HRC Injection 37
5.8 Summary of BIOMOC Findings 38
6.0 Conclusions 41
7.0 Recommendations 43
8.0 References 45

Figures

Figure 1. Building 100 Pilot Test Areas 51
Figure 2. Injection and Monitoring Location at Pilot Test Area 0514 52
Figure 3. Injection and Monitoring Locations at Pilot Test Area 0526 53
Figure 4. Injection and Monitoring Locations at Pilot Test Area S73C 54
Figure 5. Sum of Organic Acid Concentrations Observed at Well 0514 During the Bioremediation Pilot Test 55
Figure 6. Simulation Area Near Monitor Well 0514 55
Figure 7. Total Organic Acid Concentrations at Monitoring Well 0514 During the Pilot Test 56
Figure 8. Simulated Organic Acid Concentrations (mg/L) Two Months After HRC Injection 56

Figure 9. Simulated Organic Acid Concentrations (mg/L) 6.5 Months After HRC Injection..... 57
Figure 10. Dissolved Oxygen Concentrations at Monitor Well 0514 During the Pilot Test..... 57
Figure 11. Dissolved Iron Concentrations at Monitor Well 0514 During the Pilot Test..... 58
Figure 12. Dissolved Sulfate Concentrations at Monitor Well 0514 During the Pilot Test 58
Figure 13. Simulated Sulfate Concentrations (mg/L) Two Months After HRC Injection..... 59
Figure 14. Simulated Sulfate Concentrations (mg/L) 6.5 Months After HRC Injection..... 59
Figure 15. Dissolved Methane Concentrations at Monitor Well 0514 During the Pilot Test 60
Figure 16. Simulated Methane Concentrations (mgL) 6.5 Months After HRC Injection 60
Figure 17. Dissolved cis-DCE Concentrations at Monitor Well 0514 During the Pilot Test..... 61
Figure 18. Simulated cis-DCE Concentrations (mg/L) Nine Months After HRC Injection..... 61
Figure 19. Dissolved trans-DCE Concentrations at Monitor Well 0514 During the Pilot Test ... 62
Figure 20. Simulated trans-DCE Concentrations (mg/L) Nine Months After HRC Injection 62
Figure 21. Dissolved Vinyl Chloride Concentrations in Monitor Well 0514 During the Pilot Test 63
Figure 22. Simulated Vinyl Chloride Concentrations (mg/L) Nine Months After HRC Injection 63
Figure 23. Dissolved Ethene Concentrations in Monitor Well 0514 During the Pilot Test 64
Figure 24. Predicted Organic Acid Concentrations (mg/L) One Year After HRC Injection 64
Figure 25. Predicted cis-DCE Concentrations (mg/L) One Year After HRC Injection 65
Figure 26. Predicted Vinyl Chloride Concentrations (mg/L) One Year After HRC Injection..... 65

Tables

Table 1. Chemical Species Included in the BIOMOC Model 25
Table 2. Initial and Boundary Conditions Adopted in the Transport Portion of the BIOMOC Model..... 25
Table 3. Biologically Mediated Reactions Simulated in the BIOMOC Model 26
Table 4. Biodegradation Processes, the Solutes Involved in Each Process, and the Microbial Population Responsible for Each Process in the Area 0514 Simulation 27
Table 5. Uptake Coefficients Used in the BIOMOC Model of the Area 0514 Pilot Test 28
Table 6. Monod and Biomass Growth Parameters Used in the Calibrated BIOMOC Model..... 32

1.0 Introduction

The modeling described in this report was conducted to simulate the effects of enhanced bioremediation pilot testing currently underway in the surficial aquifer at the Building 100 Area at the Young - Rainey Science, Technology, and Research Center (STAR Center) in Largo, Florida. It is anticipated that the types of models produced under this study will be used to help predict the benefits of full-scale enhanced bioremediation actions for ground water not only in the Building 100 Area, but also at other sites on STAR Center property. The contaminants being considered in this study are chlorinated ethenes, which are also referred to as chloroethenes. As discussed in subsequent sections of this document, a model of one of the pilot test locales can potentially aid the design and costing of future remediation systems for chloroethenes like dichloroethene (DCE) and vinyl chloride (VC), and facilitate subsequent evaluation of remediation system progress.

The model simulations presented herein focus on ongoing pilot testing based on the injection of Hydrogen Release Compound (HRC), a product of the firm Regenesis (2003a, 2003e). HRC has been injected into the local shallow aquifer (surficial aquifer) near Building 100 using temporary direct push technology-boreholes. According to Regenesis literature, HRC slowly releases lactic acid, which in turn breaks down to other organic acids, including acetic acid, and dissolved hydrogen [$H_{2(aq)}$]. Acetic acid and hydrogen are used by bacteria in the ground water (McCarty 1997) in respiration processes that can lead to biodegradation of the chlorinated solvent contaminants like trichloroethene (TCE), isomers of DCE, and VC. The degradation of these compounds comprises a chemical sequence referred to as reductive dechlorination, or reductive dehalogenation. Dechlorination refers to the replacement of chlorine atoms in the chlorinated ethenes with hydrogen atoms. Reductive dechlorination occurs mostly under anaerobic conditions, i.e., where micro organisms can live and grow in the absence of free oxygen.

It is significant that the dehalogenation brought on by HRC application is, in a chemical sense, reductive. Other biological mechanisms that sometimes lead to DCE and VC degradation comprise the opposite of reduction in a process referred to as oxidation (Bradley 2000; Chapelle et al. 2003). Past studies at the STAR Center (e.g., DOE 2003a; Xpert Design and Diagnostics 2003) have indicated that chemical conditions in the surficial aquifer are generally not conducive to biodegradation of DCE and VC by oxidation.

Before enhanced reductive dechlorination of DCE and VC can occur in ground water, the acetic acid and H_2 generated by HRC will react with constituents that occur naturally in the subsurface. These pre-dechlorination reactions, each of which is mediated by a specific form of subsurface bacteria, involves an exchange of electrons between chemicals. Specifically, the acids and dissolved H_2 act as electron donors, while the naturally occurring chemicals reacting with them become electron acceptors. Chemicals that can act as electron acceptors include dissolved oxygen [$O_{2(aq)}$], nitrate (NO_3), manganese (Mn^{4+}), solid-phase iron (ferric iron, or Fe^{3+}), dissolved sulfate (SO_4), and carbon dioxide (CO_2). As the sequence of reactions between acetic acid or hydrogen and these electron acceptors progress, the ground water in which they take place becomes more chemically reducing, and the potential for chlorinated ethenes to act as the acceptors of electrons donated by the acetic acid and H_2 increases. The intent of enhanced bioremediation using substances like HRC is to produce a chemical environment that is sufficiently reducing to speed up these latter reactions, particularly reactions involving DCE and

VC. In doing so, populations of bacteria specifically capable of generating energy as part of the dechlorination process begin to grow.

An earlier, preliminary modeling study of bioremediation at the site (DOE 2003b) primarily examined (1) the distribution of HRC in the surficial aquifer as a result of its injection into the subsurface, and (2) potential spreading of HRC-derived acids due to advection, mechanical dispersion, and molecular diffusion. An issue that was closely examined during the previous modeling was a relatively large aqueous-phase diffusion coefficient that Regenesis (2003d) reported as being applicable to the acids generated from HRC breakdown. The diffusion coefficient was considered a key parameter because it could have a significant effect on the ability of acids to spread to all portions of the aquifer such that widespread enhanced bioremediation could be achieved. Though no absolute conclusions were drawn from the earlier simulations regarding diffusion potential, evidence was presented indicating that the actual diffusion coefficient would be much lower than the Regenesis-published coefficient, and that reductive dechlorination would be correspondingly limited.

Though attempts were made during the earlier modeling study to account for the bacterially-mediated reaction of acetic acid and dissolved hydrogen with VC, the modeling techniques used at the time were considered primitive and incapable of capturing all relevant chemical reactions. One of the shortcomings of the model produced at the time was that it could not account for the reaction of acetic acid and H_2 with natural electron acceptors. Consequently, a recommendation was made that more detailed modeling be conducted that fully accounts for the reactive transport of all chemicals involved in the transformation of acetic acid and H_2. Such a model would only allow dehalogenation of chlorinated ethenes to occur after the needs of other electron acceptors had been met. A computer code capable or meeting this objective was not available during the earlier study. Since that time, however, a numerical simulator of biodegradation (BIOMOC) developed by the U.S. Geological Survey (USGS) has been found that suits the project's needs. This document reports the features of the modeling software and how it has been used to help explain observations that have been made during the past several months at pilot test plots where HRC has been applied. The results of this new modeling investigation suggest that potential bioremediation of dissolved organic contaminants in the surficial aquifer underlying the STAR Center can be adequately described and quantified, and most likely predicted.

2.0 Background

2.1 Pilot Testing

The pilot tests for evaluating the efficacy of HRC release in promoting biodegradation of chlorinated ethenes at the Building 100 Area began in March of 2003. Injection was conducted in three separate areas, each of which is identified by a single monitoring well associated with the test (Figure 1). Nine temporary direct push technology injection boreholes, consisting of three rows of three, were used in each location. The borehole rows were located approximately parallel to the ambient ground water flow direction, which is toward the southeast.

The three test locations are distinguished from each other by the spacing used between the rows of injection boreholes. The spacing is approximately 10 feet (ft) in the vicinity of monitoring well 0514, which is located about 20 ft east of Building 100 (Figure 2). Twelve-foot spacing is used near well 0526, which is located in the middle of the parking lot east of Building 100 (Figure 3). The third test area, situated around well S73C (Figure 4), makes use of 15-ft spacing between the injection boreholes. Background information regarding the pilot tests' original design, the ultimate configuration of injection boreholes in each test area, and the manner with which HRC injection was accomplished are presented in the remediation plan generated by the bioremediation contractor SEC (2003a,b).

The concentrations of several dissolved constituents have been measured in ground water samples collected from each of the three monitoring wells since the tests began. These concentrations have been compared with baseline concentration data from March 11, 2003, and used for several purposes, the most important of which are to (1) develop a preliminary assessment of the degree to which organic acids generated by breakdown of the injected HRC spread through the aquifer and (2) assess the capacity of produced acetic acid and dissolved hydrogen to act as electron donors in the biotransformation of the contaminants DCE and VC. Additional benefits drawn from analysis of the data include identification of the most important biologically mediated reactions between the proton donors and natural electron acceptors in the aquifer and, as a result, the aquifer's capacity to reach more chemically reducing conditions.

To date, about 12 months after the baseline sampling, the results from six sampling events spread over a ten-month period are available. Not surprisingly, the findings stemming from analyses of the concentration data have varied between the pilot test areas. Some of these differences can be attributed to the different distances used between injection boreholes in the three areas, whereas others are due to differences in the location of the single monitoring well used at each area. Such differences in test observations point out the importance of advective and dispersive transport processes in affecting bioremediation as well as the bacterially-driven chemical reactions that must take place if enhanced bioremediation is to be successful. The modeling study that is the subject of this report has helped to better quantify those transport processes, and has identified a need for continued and more extensive monitoring.

Much of the data interpretation performed thus far focuses on the well 0514 test area since the greatest influence on aquifer chemistry has been observed in this area. Accordingly, the modeling conducted for this investigation has been concentrated on the 0514 area. In Section 3.2 of this report, current assessment of well 0514 results is used to preliminarily interpret some results from the other pilot test areas. In later chapters, the findings from a biotransformation

model of the 0514 area are applied to refine the interpretations and to predict what can be expected in the future at the other areas.

2.2 Previous Modeling

As mentioned earlier, previous simulation of the enhanced bioremediation efforts at Building 100 (DOE 2003b) focused on two general types of processes:

1. Advective movement of HRC away from injection sites, and
2. The spatial distribution of organic acids produced by the breakdown of injected HRC and subsequently affected by combined advective, dispersive, and diffusive transport processes.

The first of these process types was expected to generally occur in radial directions away from the injection locations. The second type took into account the spreading of organic acids as they moved downgradient under ambient ground water flow conditions. Based on information in the scientific literature, it was believed at the time of the previous modeling that dechlorination of DCE and VC could be partially or completely accomplished if the acids were capable of spreading widely within the surficial aquifer.

Initial simulations with the previous model examined the influence of aquifer porosity and the aqueous diffusion coefficient on organic acid distribution over space and time. Because the effects of preferential flow were at the time believed to affect this distribution, several simulations were conducted using effective porosities that were considerably smaller than the surficial aquifer's actual porosity. Though this approach made it possible for simulated acid to propagate downgradient to monitor wells faster than would occur if preferential flow paths were not present, it also meant that organic acid plumes generated by the model and extending downgradient of HRC injection sites were not truly representative of actual plumes. This is because, in the field, much of the area covered by the model-generated plumes would actually comprise lower permeability zones, wherein influx of acid would be limited to non-existent and, consequently, little to no dechlorination activity would be expected.

To further analyze the potential obstacles brought on by preferential flow, additional simulations were conducted using the relatively large diffusion coefficients that Regenesis (2003d) ascribes to lactic acid produced by the degradation of HRC. Though these latter model runs suggested that the resulting diffusion rates would allow organic acids to better penetrate low-permeability zones, the model developers remained skeptical that these diffusion rates were realistic and applicable to the Building 100 pilot tests. This skepticism stemmed partly from the fact that published values of the diffusion coefficient of all solutes in free water, including those for organic acids, are generally about two orders of magnitude less than the Regenesis-published value. In addition, the Regenesis experiment concerning lactic acid diffusion was performed in a column and, consequently, did not take into account radial transport away from an injection borehole (i.e., radial diffusive transport is slower than one-dimensional, linear diffusion).

The RT3D code (Clement 1998) was used during the previous modeling in attempts to simulate dechlorination of chloroethenes. This simulator was selected because the modules incorporated within its publicly-distributed versions account for both first-order and zero-order reactions. However, it was ultimately concluded that neither of these reaction types was adequate for describing the sequence of terminal electron acceptor processes (TEAPs) that acetic acid and

dissolved H_2 experience, both leading up to and during dechlorination activity. In an effort to account for the time delay between introduction of HRC and dechlorination of DCE and VC, a generic substance referred to as "organic acid" was allowed to first undergo transport as affected by advection, dispersion, and first-order degradation for a prescribed period of time. Degradation in this case was assumed to approximate the uptake of acetic acid and H_2 by natural electron acceptors. Subsequent to the initial prescribed time period, organic acid was then assumed to degrade chlorinated ethenes instantaneously. This latter step required the use of a stoichiometric coefficient describing the number of moles of chlorinated ethene degraded for each mole of organic acid present.

Though the previous modeling of bioremediation at the Building 100 Area helped shed light on the potential migration of organic acids released from HRC injection sites, it fell far short of providing a comprehensive simulation tool capable of matching observed concentrations of all reactants affected by the acid migration and H_2 production. Specifically, it was incapable of accurately simulating (1) declining concentrations of electron acceptors potentially reacting with acetic acid and H_2 (e.g., oxygen, nitrate, solid-phase manganese, ferric iron, sulfate, TCE, DCE, VC) and (2) increasing concentrations for transformation products of these reactions (e.g., ferrous iron, methane, ethene). Of particular concern was the use of the instantaneous reaction module in RT3D to simulate the reduction of VC to ethene after an arbitrarily prescribed lag time. This approach essentially allowed reductive dechlorination of VC to take place completely independent of all reactions that must occur before the dehalogenation process can start. Moreover, the single stoichiometric coefficient used to describe the instantaneous decrease in concentration of a chlorinated ethene in response to a predicted organic acid concentration was not based on an actual biologically-mediated chemical reaction. Consequently, the coefficients used were groundless.

2.3 Recommended Second Phase of Modeling

Because of the shortcomings of the previous model, it was recommended that future simulations be conducted with a model that would

- account for all electron acceptors individually, rather than lumping nitrate, manganese, iron, sulfate, and others, into a single group; and
- appropriately simulate the kinetics of the reactions involved rather than resorting to either instantaneous reaction or first-order decay approximations.

At the time, a customized version of RT3D was the only code that the authors were aware of that would be able to meet these needs. However, access to this code would have required purchase of the services of the code developers at Pacific Northwest National Laboratories (PNNL). Fortunately, in the months following the previous modeling effort, a bioremediation simulator that was capable of meeting the site's modeling needs and was free-of-charge from the USGS was found. This code, BIOMOC (Essaid and Bekins 1997), is the simulator that is used in this second phase of modeling.

End of current text

3.0 Biotransformation of Chlorinated Ethenes in Ground Water

3.1 General History

The use of amendments to enhance bioremediation of chlorinated solvents in ground water is discussed extensively in the scientific literature. This has been especially true in the last two decades, during which many discoveries were made that shed light on the processes that play a role in the biodegradation of organic contaminants. Perhaps the most important discovery was that the complete biodegradation of compounds such as tetrachloroethene (PCE) and TCE into environmentally innocuous end products like ethene was even possible. Until the early 1990s, it was generally believed that biologically-facilitated breakdown of TCE into DCE could occur naturally but with no real benefit to the bacteria involved, and that further degradation of DCE to VC, and from VC to ethene, was either unlikely or extremely slow under most environmental conditions. A common finding at that time was that DCE and VC would tend to accumulate in ground water, and, because VC is considered a serious toxin, no significant reduction in risk could be achieved. However, when it was learned that certain bacteria existed that were capable of using DCE and VC to produce energy, the interest in finding ways to biologically transform these two chloroethenes in ground water was renewed. Since that time, more than one biologically-mediated mechanism for removing DCE and VC from ground water has been brought to light and researched. This modeling study attempts to quantify the removal of these contaminants from Building 100 ground water via one form of these mechanisms.

3.1.1 Natural Attenuation of Chlorinated Ethenes

Concentrations of chlorinated solvents dissolved in ground water can naturally attenuate due to a variety of microbial degradation processes that fall under one or more of four general categories: (1) reductive dechlorination, (2) aerobic oxidation, (3) anaerobic oxidation, and (4) aerobic cometabolism. Though engineered facets of each of these natural processes have, at one time or another, been examined for their applicability to or actually applied to the surficial aquifer at the STAR Center, it now appears that reductive dechlorination stands the greatest chance of reducing concentrations of DCE and VC to levels that are below applicable cleanup standards. To provide a basis for the logic behind the Building 100 pilot testing, this section and the following one present abbreviated descriptions of each of the natural process categories.

<u>Reductive Dechlorination</u>

As previously mentioned, microbial reductive dechorination involves the replacement of chlorine atoms in a chlorinated ethene's chemical structure with a hydrogen atom. Inherent in this process is an exchange of electrons between one chemical referred to as an electron donor and another referred to as an electron acceptor. The constituent ultimately receiving the electron is sometimes referred to as a terminal electron acceptor (TEA) because it can be at the end of a series of intermediate processes involving electron transfer. Accordingly, the associated metabolic activity is labeled a TEAP. Though chlorinated ethenes like DCE and VC can act as TEAs, they have to compete for electrons against other naturally occurring acceptors typically found in ground-water systems (McCarty 1997).

Under anaerobic conditions, the chlorinated solvent PCE, with four chlorine atoms, is generally found to readily undergo reductive biotransformation to TCE, with three chlorine atoms. This is because PCE is a more highly oxidized chemical (susceptible to reduction) relative to all of the

naturally occurring electron-accepting species found in ground water, with the notable exception of dissolved oxygen ($O_{2[aq]}$) (Chapelle et al. 2003). TCE, in turn, will degrade relatively easily to cis-1,2-DCE, with two chlorine atoms, in an anaerobic system containing bacteria referred to as iron reducers. However, the subsequent degradation of cis-DCE to VC (with one chlorine atom), and from VC to ethene (with no chlorine atoms) is less likely to occur under natural conditions. Both DCE and VC are less oxidized (more reduced) than either PCE or TCE, and, therefore, show little potential to undergo further biologically induced chemical reduction.

As a result of the decreasing reductive potential with decreasing number of chlorine substituents, reductive dechlorination in ground water systems is often incomplete and frequently leads to the accumulation of cis-DCE and VC. Until the early 1990s, few researchers thought it was possible to move beyond this state of accumulation. Part of the conventional thinking stemmed from the widely held belief that dechlorination was accidental and of no benefit the microorganisms facilitating the process. However, the discovery in 1993 that a group of microorganisms known as halorespirers (Bradley 2000) could produce energy using chloroethenes as TEAs led to a resurgence of ideas for promoting reductive dechlorination as a means of bioremediation. Since that time, several halorespirers capable of reducing PCE or TCE to DCE have been identified. However, the microbial populations identified thus far as being capable of carrying out reduction of higher chlorinated ethenes to VC and eventually ethene are limited to strains of the organism dehalococcoides (Chapelle et al. 2003; Major et al. 2003).

Reductive dechlorination of TCE to yield cis-DCE can apparently occur under iron-reducing (Fe^{3+}-reducing) conditions and in more strongly reducing environments. Reductive dechlorination of cis-DCE to yield VC, however, requires at least sulfate-reducing conditions (Bradley 2000). Reductive dechlorination of cis-DCE to the non-chlorinated product ethene is characteristically slow and is significant only under either sulfate-reducing or highly reducing, methanogenic conditions. This latter observation explains why many engineered bioremediation schemes for chlorinated ethenes focus on ways to generate ground water environments that are more reducing and susceptible to sulfate reduction or, in some cases, methane production.

Aerobic Oxidation

Though the tendency of chlorinated ethenes to undergo reductive dehalogenation decreases as the number of chlorine substituents decreases, the potential for oxidation of chlorinated ethenes increases with decreasing chlorine substituents. In aerobic systems, in particular, VC can degrade rapidly via an oxidation process. In some cases, VC acts as the sole carbon source for growth and metabolism of aerobes, which are microbes that use oxygen as the electron acceptor. In others, VC is degraded incidentally as aerobes oxidize a different primary substrate. This incidental breakdown of VC, which is called cometabolic oxidation, does not supply energy for microbial growth or metabolism. DCE can also be degraded in aerobic systems, either through a cometabolic process or by direct oxidation (Chapelle et al. 2003).

Unfortunately, microbial oxidation of DCE and VC under aerobic conditions is not observed in most ground water domains. The appearance of these two contaminants is often the result of reductive dehalogenation of PCE and TCE in systems that were generally anaerobic to begin with. Thus, unless the DCE and VC are eventually transported to an environment that is aerobic, such as where ground water discharges to a surface water body, the probability of naturally achieving significant decreases in the concentrations of either remains low. Attempts are sometimes made to add oxygen to ground water to stimulate aerobic biodegradation of

chlorinated ethenes in an otherwise anaerobic system, but these engineered approaches can be expensive and are sometimes impractical (Chapelle et al. 2003).

Anaerobic Oxidation

Anaerobic oxidation of DCE and VC has become accepted as a possible mechanism for natural attenuation of ground water contamination during the last decade. Studies by Bradley and Chapelle (1996; 1998) have shown that VC can degrade to carbon dioxide (CO_2) if a sufficiently strong oxidant is available to drive related microbial activity. Apparently, ferric iron (Fe^{3+}) is a sufficiently strong oxidant for VC degradation. However, it is important that Fe^{3+} be present in relatively large quantities if lasting decreases in VC concentrations are to be attained (Chapelle et al. 2003) through anaerobic oxidation.

As alluded earlier, the potential for oxidation of organic chemicals in the environment increases as those chemicals become more reduced. As a consequence, VC tends to degrade via oxidation more readily than does DCE. An instance where oxidation of DCE was shown to occur relatively rapidly, resulting in mineralization of the contaminant directly to CO_2, required the presence of solid-phase manganese (Mn^{4+}) (Bradley et al. 1998), which is considered a stronger oxidant than Fe^{3+}.

Assuming that the chlorinated ethenes with a greater number of chlorine substituents (i.e., PCE and TCE) will undergo reductive dechlorination relatively quickly, it is logical that the anaerobic oxidation of the DCE and VC resulting from such dechlorination provides a viable natural attenuation pathway under certain conditions. In particular, for this combination of microbial degradation mechanisms to be successful, the presence of Fe^{3+} and Mn^{4+} in relatively large quantities is required. The success of anaerobic oxidation of DCE and VC also depends on the presence or lack thereof of other organic constituents that serve as electron acceptors, such as petroleum-derived hydrocarbons. These latter types of organic contamination tend to be more reduced than either DCE or VC and thus compete for electron donors more efficiently (Chapelle et al. 2003).

Aerobic Cometabolism

A wide variety of aerobic microorganisms have been identified that are able to oxidize TCE, DCE, and VC to CO_2 when in the presence of other organic chemicals. These organisms include methane oxidizers, propane oxidizers, and aromatic compound oxidizers (Bradley 2000). The chlorothene oxidation occurring in these instances does not supply energy for microbial growth or metabolism; rather, the responsible microorganisms use oxygen in the process of degrading the other organic chemical(s), and chloroethenes are fortuitously degraded in the process. Hence this transformation of chlorinated ethenes to CO_2, without any toxic intermediate products, is referred to as aerobic cometabolism.

The conditions suitable for cometabolic degradation of chloroethenes are rarely observed in the interior of ground water contaminant plumes containing them. This is because the chloroethenes are typically associated with anaerobic conditions, particularly under the environments associated with reductive dechlorination of PCE and TCE and concomitant buildup of DCE and VC.

3.1.2 Enhanced Reductive Dechlorination of Chlorinated Ethenes

Some enhanced bioremediation actions for chlorinated solvents and their transformation products are based on schemes designed to promote oxidation of chlorinated solvents. Occasionally, these schemes attempt to take advantage of the cometabolic degradation of DCE isomers and VC, either through the addition of co-substrates or the use of ambient non-solvent contaminants. However, some of the more promising approaches to chloroethene degradation during the past decade have focused on the use of aquifer amendments that attempt to chemically reduce a ground water system such that sulfate-reducing or methanogenic conditions conducive to reductive dechlorination of DCE and VC are created. The types of amendments applied in these latter cases vary from organic acids to methanol, alcohols, and other organic substrates.

Typically, the chemical amendments added to an aquifer to enhance reductive dechlorination take part in a series of reactions before producing the strongly reducing conditions adequate for the degradation of DCE and VC. Some of these reactions produce the electron donors acetic acid and hydrogen (NRC 2000). Subsequently, the acetic acid and hydrogen undergo a series of biologically mediated reactions with natural electron acceptors. These reactions, with regard to electron acceptor, proceeds from the most thermodynamically favorable to the least favorable:

Oxygen (O_2)>Nitrate (NO_3)>Manganese (Mn^{4+})>Iron (Fe^{3+})>Sulfate (SO_4)>Carbon Dioxide (CO_2)

In ground water systems, some of these reactions tend to be insignificant in comparison to others.

A specific type of microorganism facilitates each one of the reactions (NRC 2000) between the acetic acid and H_2 and electron acceptors. The last reaction prior to reductive dechlorination of DCE and VC, CO_2 reduction, is facilitated by methane producing bacteria. It is not necessarily required that one electron acceptor be fully consumed before the next reaction in the sequence can proceed; some biotransformation reactions can occur simultaneously.

The HRC used in the Building 100 area pilot tests is described as a high viscosity liquid that undergoes a series of fermentation reactions to produce multiple organic acids and dissolved hydrogen (Regenesis 2003b, 2003c). The first acid formed is lactic acid (Regenesis 2003e). The high viscosity of HRC is purportedly advantageous because it helps to slow down the generation of lactic acid, and, subsequently, the acetic acid and H_2 required for reductive dechlorination. Such slow production of electron donor material also apparently helps to maintain relatively low H_2 concentrations, which, according to some investigators (Fennel et al. 1997; Yang 1998) helps dechlorinating organisms to compete more effectively against other microbial populations (e.g., methanogens) for available electrons.

Monitoring of dissolved H_2 as part of enhanced dechlorination efforts not only helps to assess the degree to which this electron donor has become available, but also to identify which TEAPs are predominant at different times (e.g., Vroblesky and Chapelle 1994). Hydrogen concentrations tend to be smallest during nitrate and iron reduction, and highest under methanogenic conditions (Chapelle et al. 2003). Thus, researchers tend to seek methods for inducing sulfate reduction, or possibly methagonesis, while keeping H_2 concentrations relatively low (e.g., Fennel et al. 1997).

3.1.3 Implications of Bioremediation Processes for the STAR Center

Chemistry data collected from the surficial aquifer during the past decade suggest that biodegradation of chlorinated solvents dissolved in ground water has been occurring naturally at the site. Predominant anaerobic conditions observed in the aquifer indicate that reductive dechlorination processes have promoted this degradation, resulting mostly in decreases of PCE and TCE concentrations. However, as is typical of many ground water systems, this degradation has led to a buildup of DCE and VC in many parts of the surficial aquifer underlying the STAR Center, including the Building 100 Area. Subsequent degradation of DCE and VC under natural conditions appears to be extremely slow. This problem is exacerbated at the Building 100 Area because it is likely that continuing sources of chloroethenes exist below the building (DOE 2002) in locales that cannot, at this time, be reached for remediation.

The continuing occurrence of VC in the Building 100 Area presents a potential health risk. Ambient VC concentrations tend to consistently hover around values of 40 to 50 micrograms per liter (μg/L), yet the EPA drinking water maximum contaminant level (MCL) for this compound is 2 μg/L, and its state of Florida regulatory standard at the STAR Center is 1 μg/L. Such observations infer that natural attenuation of the less chlorinated solvents via anaerobic oxidation is not a viable remedial alternative for the site. Consequently, engineered methods are needed to help drive VC levels lower, as well as the concentrations of DCE isomers that potentially degrade into VC.

Attempts were made in previous years using a biosparge system to enhance degradation of TCE, DCE, and VC in the surficial aquifer at the 4.5 Acre Site, which is located adjacent STAR Center property. The system, consisting of three horizontal wells connected to blowers, began operation in November 1999 and was shut down in mid-2003. Monitoring of VC concentrations at the site during this period indicated that this contaminant continued to persist at levels close to those observed prior to remediation (1 to 5,000 μg/L).

The primary intended means of aquifer remediation using the biosparge system was aerobic oxidation, wherein the growth of aerobic bacteria would be promoted while DCE and VC were degraded. However, two studies aimed at evaluating remediation performance at the 4.5 Acre Site (DOE 2003; Xpert Design and Diagnostics 2003) indicated that sparging was unsuccessful at creating the aerobic conditions necessary for this approach to be viable. Problems contributing to the lack of success included an excessively large chemical oxygen demand in the aquifer and the propensity for preferential flow paths to form in the subsurface during air injection. The latter of these problems provided some indication that preferential flow would likely be observed under any form of enhanced bioremediation.

When the biosparge system first began operation in late 1999, it was believed that cometabolic oxidation processes would help contribute to significant declines in local chloroethene concentrations due to the presence of toluene in local ground water. Recently, Fournier (2003) inferred that the cometabolism occurring at the site during early stages of biosparge operations had comprised a successful bioremediation effort. However, measured concentrations of DCE isomers and VC at the site during the past few years tend to belie this interpretation.

At this stage of the cleanup process at the STAR Center, it seems unlikely that in situ oxidation of chlorinated ethenes in the surficial aquifer will be successful. For oxidation to show any significant removal of DCE and VC mass from the aquifer, ponds at the site, whether existing or

constructed in the future, would probably have to be utilized to induce discharge of ground water toward surface water bodies where more oxidizing conditions could be achieved (e.g., Chapelle et al. 2003). Short of engineering such an approach, however, it seems that enhanced reductive dechlorination stands a better chance of achieving remediation goals. Some measure of success was achieved when this remediation method was tested at another site on STAR Center property (the Northeast Site) in the late 1990s (DOE 1998). One of the difficulties encountered during the test, however, was the tendency for applied bioremediation amendments to be affected by preferential flow in the subsurface.

3.2 Monitoring Results at the Building 100 Area

Ground water monitoring over the first 10 months after pilot test initiation has indicated distinctive changes in the concentrations of dissolved constituents. The most noticeable trends have been observed in well 0514, where both the organic acids produced by the degradation of HRC and indicators of chemically reducing conditions have been observed during most of the monitoring period. These conditions have also been identified at wells 0524 and S73C, albeit at later times and to a lesser degree than at well 0514.

3.2.1 Identification of Reactants

The identification of natural electron acceptors reacting with organic acids and hydrogen first required an assessment of whether the acceptors were present in the surficial aquifer at the site. Examination of baseline concentrations collected during the pre-test sampling event on March 11, 2003, indicated that oxygen, ferric ion, and sulfate would fit into this category. Nitrate (NO_3) was not considered a likely electron acceptor because it was not detected in any of the pilot test monitor wells, both prior to and during the tests. Similarly, little evidence existed to suggest that solid-phase manganese (Mn^{4+}) is acting as a natural electron acceptor. Dissolved manganese (Mn^{2+}) concentrations in the three test areas have remained low, ranging between 10 and 20 μg/L throughout the testing.

Dissolved methane was detected at all three monitor wells on March 11, 2003, at concentrations ranging from about 300 to 500 μg/L. The presence of this latter constituent suggested that chemically reducing conditions are observed under background conditions within the aquifer such that methane-producing bacteria (methanogens) respire and generate energy. The natural electron acceptor that is contributing to methane generation under background conditions is carbon dioxide (CO_2) (Chapelle et al. 2003).

Identification of dissolved oxygen (DO) as a natural electron acceptor capable of reacting with organic acids generated from HRC was considered somewhat surprising. Previous studies at the 4.5 Acre Site (e.g., DOE 2003a; Xpert Design and Diagnostics 2003) northwest of Building 100 had indicated that it is very difficult to convert the surficial aquifer into an aerobic system, i.e., a system characterized by relatively high levels of dissolved O_2. Nonetheless, DO was observed prior to the start of pilot testing in well 0514 at a concentration of about 0.8 milligrams per liter (mg/L), and in well 0526 at a level of about 4 mg/L (the DO level in well S73C was 0.19 mg/L). Under most environmental conditions, the solubility of dissolved O_2 is considered to be about 10 mg/L; thus, concentrations of 1 to 4 mg/L represent about 10 to 40 percent, respectively, of the saturated level for this constituent. Within a month of the start of pilot testing, DO levels in wells 0514 and 0526 had dropped below 0.2 mg/L, and subsequently remained below their pre-test values for the following 9 months. The likely cause of this decrease is a reaction between

oxygen and HRC-derived organic acids that is facilitated by oxygen-using bacteria (i.e., aerobes or facultative anaerobes.

The evidence for ferric iron (Fe^{3+}) acting as a natural electron acceptor is indirect. Attempts to measure soil concentrations of this solid-phase component had indicated that only very small amounts of ferric iron were available to microorganisms. Yet levels of dissolved ferrous iron (Fe^{2+}) in the aquifer during baseline sampling were relatively high, possibly indicating the production of the latter under background conditions by iron-reducing bacteria. As discussed in a subsequent section, the increase in Fe^{2+} concentrations expected from enhanced iron reduction due to the presence of acetic acid and hydrogen has not been observed in the pilot test areas. To the contrary, dissolved iron concentrations noticeably decrease in the presence of acetic acid and H_2. This observation in turn implies a reaction between Fe^{2+} and another dissolved constituent that causes the dissolved iron to precipitate out of solution. It is highly likely that sulfide reduced by sulfate-reducing bacteria is the other constituent reacting with dissolved iron to form the precipitate. Regardless of the nature of that reaction, strong correlation of changes in dissolved iron with the introduction of a bioremediation amendment indicates that iron reduction is ongoing and affected by the pilot tests.

3.2.2 Observed Trends

Organic Acids

The concentrations of five organic acids — lactic acid (lactate), pyruvic acid (pyruvate), butyric acid (butyrate), propionic acid (propionate), and acetic acid (acetate) — have been monitored in the pilot test area monitor wells, both prior to commencement of the tests and during all six subsequent sampling events over a 10-month period. Dissolved hydrogen ($H_{2[aq]}$), however, has not been monitored. Thus, with the available data, it has been possible to develop some measure of the mass of organic material that has been available to fermenting bacteria for the production of H_2, but an accurate measure of the combined mass of acetate and H_2 available to electron acceptors in the surficial aquifer has not been achievable. Consequently, the summed concentrations of the organic acids, by themselves, have been used to provide insight into the transport processes and chemical reactions occurring in the test areas.

Under baseline conditions on March 11, 2003, none of the above-mentioned organic acids was detected in the test areas. The detection limits for the acids were set relatively high for the purpose of clearly identifying their presence as a result of HRC degradation and subsequent transport with ambient ground water flow.

Since commencement of the tests, some organic acids have been detected in measurable quantities at monitor wells in the three test areas. However, the types of acids detected, their measured concentrations, and the frequency of their detection have varied between testing locations. The most noticeable, most frequent, and long-lasting detections have been made at well 0514, where design spacing between injection wells (~ 10 ft) is smallest. Acetate, propionate, and butyrate were all detected at measurable levels in this well during the second sampling event, which fell within 3 months of the test start and some during subsequent events. However, butyrate was not detected during the fifth sampling that occurred on November 18, 2003, and none of the acids were detected in the middle of January 2004, about 10 months after the test started. With the exception of the fourth sampling event on September 23, 2003, when pyruvate was estimated at a level of less than 100 mg/L,

concentrations of this acid at well 0514 have continually been below the detection limit adopted for this compound (10 mg/L).

Curiously, lactate, the first organic acid produced by degradation of HRC (Regenesis 2003b), has not been identified in ground water. A possible explanation for this latter observation is that virtually all lactate stemming from the breakdown of HRC in the upgradient injection location closest to 0514 has already been acted upon by fermenting bacteria to produce other organic acids before reaching this well. Alternatively, it is possible that the detection level for lactate may have been too high to allow for measurement of this acid's concentration, which, at the monitor well, was probably much lower than that occurring in the immediate vicinity of the HRC injection.

Tracking of the summed concentrations of all monitored acids in the 0514 area during some months suggests that the products of HRC degradation have been decreasing at well 0514, which in turn suggests that the influx of acetate and H_2 to the well area is gradually coming to an end. This concept is illustrated in Figure 5, which shows temporal changes in the summed concentrations of pyruvate, butyrate, propionate, and acetate at well 0514 during the pilot test. This graph suggests that a little over a month was required for HRC-derived acids to first reach the well from the closest upgradient HRC injection point, and that the maximum total organic acid concentration at 0514 occurred about 6 months after the injection. Since the time of peak concentration, the summed organic acid concentrations have dropped off relatively rapidly, reaching a value of close to zero between 8 and 10 months after injection.

Because the graph of total acid concentration versus time since injection (Figure 5) fails to completely describe the concentration of dissolved H_2 during the pilot test, it is not a complete reflection of the availability of electron donors produced by the breakdown of HRC. That is, it is possible that hydrogen still exists in the aquifer near well 0514 some 8 to 10 months after injection, and that H_2 is maintaining a capability to not only react with natural electron acceptors, but also with DCE isomers and VC. Some evidence of this latter possibility is presented in the next section regarding observations of oxidation-reduction potential (ORP).

Oxidation-Reduction Potential

Monitoring of ORP in the test areas has shown that reactions between transformation products of HRC degradation and natural electron acceptors create a ground water system that is more anaerobic than under background conditions and, accordingly, more chemically reducing. During baseline sampling, ORP values in the monitor wells ranged from a high of 29 millivolts (mV) (in well 0514) to a low of –18 mV (in well 0526). Such values suggested that the ground water system under background conditions tended to be mildly reducing. Between 1 and 2 months after the start of the pilot tests, ORP values began decreasing significantly in all three test areas, approaching values close to –300 mV in the 0514 area. Since this initial drop, ORP values in well 0514 have, for the most part, remained quite low, indicating the possibility that dissolved H_2 continues to react with system electron acceptors. A similar persistence of low ORP in well 0526 also supports this possibility. In contrast, however, ORP numbers in well S73C dropped to as low as –168 mV about 3 months after injection of HRC, and subsequently began increasing to pre-test levels of about –5 mV. This latter result suggests that the capacity of HRC to drive the ground water system to a more reducing state in the vicinity of well S73C may have already passed. Alternatively, it is possible that the wider spacing used between injection boreholes at

this location (~ 15 ft) has minimized the amount of acetic acid and dissolved H_2 that reach well S73C.

Natural Electron Acceptors

In addition to decreases in ground water O_2 levels, declines in dissolved SO_4 concentration have been observed in the 0514 area since the start of the pilot testing. The latter of these trends can be attributed to the conversion of sulfate to sulfide via reactions controlled by sulfate-reducing bacteria. During baseline sampling on March 11, 2003, dissolved sulfate in well 0514 was observed at a level of about 150 mg/L; during and subsequent to the second sampling event, sulfate levels have ranged between about 10 and 100 mg/L. In accordance with the order in which electron acceptor activity is normally observed, the decrease in sulfate concentration appears to have lagged the observed decrease in dissolved oxygen levels by a month or two.

As previously discussed, no direct evidence exists for the transformation of solid-phase ferric iron (Fe^{3+}) to dissolved ferrous iron (Fe^{2+}) by iron-reducing bacteria. When this transformation takes place, concentrations of Fe^{2+} often increase in ground water. However, in lieu of an increase, Fe^{2+} levels have declined at well 0514, which is potentially indicative of additional chemical reactions involving the Fe^{2+} ion. Other means of identifying iron reduction, such as the identification of solid-phase constituents containing Fe^{2+} in affected soils may help to identify such reactions. It may be possible to quantify the degree to which iron-reducing bacteria are active at the site. It is likely that some ferric iron is available for bacterial respiration and should be taken into account when simulating bioremediation processes in the surficial aquifer.

Evidence of increased activity of methane-producing bacteria has been documented at the 0514 site during the pilot tests. Before pilot testing began, dissolved methane (CH_4) concentrations in the well were close to 0.3 mg/L; between the third and sixth sampling events, measured CH_4 levels at 0514 exceeded 1.5 mg/L and were as large as 11 mg/L. As expected, methane production has lagged behind the initiation of sulfate reduction.

Concentrations of the natural electron acceptors O_2 and SO_4 at well 0514 during the two most recent samplings have shown an increasing trend that possibly indicates the influx of ground water that is no longer affected by the presence of organic acids and H_2. The observed increase in O_2 and SO_4 levels appears to be correlated with the decline in the summed concentrations of all organic acids. In contrast to late-term trends in dissolved O_2 and SO_4 concentrations, methane (CH_4) concentrations at well 0514 showed a distinct decline between the fourth and sixth sampling events (between the sixth and tenth months of the test), indicating a decline in the activity of methanogenic organisms. Such observations provide additional evidence that HRC in upgradient injection locations has been mostly degraded, and is no longer producing acetic acid and H_2 at levels that are sufficient to meet all electron acceptor needs.

Chlorinated Ethenes

Decreases in the concentrations of DCE isomers and VC at pilot test locations over the first 10 months of the testing have been modest at best, and, in the case of trans-DCE, may not have occurred at all. Under the baseline conditions of March 11, 2003, the cis-DCE concentration at well 0514 was close to 0.04 mg/L. Since that time, cis-DCE levels have dropped slightly below a value of 0.010 mg/L, but have gone no lower. Similarly, VC, with a measured baseline concentration of about 0.05 mg/L, has failed to drop to levels below 0.02 mg/L between the firth

and tenth month of the pilot test. The reductive degradation of cis-DCE to VC might partly explain why VC levels have not declined as quickly as hoped. The relatively mild drops in chloroethene concentrations at well 0514 are somewhat discouraging given that the chemically-reducing conditions created at this locale have persisted over several months.

As a consequence of the apparently modest effects of HRC injection on chloroethene contamination, concentrations of VC in well 0514 remain above both the MCL for this constituent (0.002 mg/L) and its applicable state of Florida regulatory standard (0.001 mg/L). On the other hand, the concentration of cis-DCE at well 0514 is below its applicable MCL (0.07 mg/L) and has been since the test start. Nevertheless, the tendency for cis-DCE to be only partly degraded is detrimental because it is still available to contribute to the mass of dissolved VC.

Though organic acids have also been detected in the monitor wells for the 0526 and S73C test areas, concomitant reductions in cis-DCE and VC concentrations, if they have occurred at all, are imperceptible. For example, VC levels at wells 0526 and S73C have tended to remain close to values of about 0.003 and 0.010 mg/L, respectively, since March 2003.

Unlike cis-DCE, trans-DCE concentrations at the 0514 monitor well have remained virtually unaffected by the presence of measurable organic acids and the local creation of chemically reducing conditions. Prior to starting the pilot tests, trans-DCE was measured at a dissolved level in well 0514 of about 0.04 mg/L. Though measured concentrations of this constituent during sampling events in the succeeding 10 months dropped to as low as 0.022 mg/L, no conclusive evidence could be found to indicate that this decrease was the result of HRC injection.

Since most natural attenuation of TCE via reductive dechlorination produce cis-DCE as a transformation product (Bradley 2000; Chapelle et al. 2003), it is possible that trans-DCE occurring in the surficial aquifer today stems from past on-site use of this compound as a solvent. Observations of its relatively constant concentration during the pilot testing suggest that its chemical structure may cause it to be recalcitrant to microbial transformation.

4.0 Modeling Approach

As previously mentioned, the model produced for this study focused on reactive transport in the 0514 pilot test area. The USGS simulator BIOMOC was applied in an attempt to match observed concentrations of key solutes in well 0514 over the past 10 months. Development of the model involved several steps, including preparation of a ground water flow model, determination of representative values for parameters affecting advective-dispersive transport in the surficial aquifer at the site, and the estimation of parameters that play a role in the biologically-mediated chemical reactions between the acetic acid and hydrogen generated by HRC and various electron acceptors in the aquifer. This report section describes general features of the BIOMOC code and the mathematical formulations upon which it is designed so that the reader can ascertain the types of parameters that were used to conduct the simulations of flow and transport in the 0514 area.

4.1 BIOMOC Code

BIOMOC was developed through modifications of an existing numerical ground water transport model based on the method of characteristics (MOC) (Konikow and Bredehoeft 1978). Though the original MOC simulator was only capable of simulating transport of a single chemical constituent, BIOMOC, because of its ability to simulate reactive transport, can handle the transport of several constituents. In addition, the modified code accounts for several different reactions involving the various chemical species, and a different microbial population for each reaction.

Before transport of dissolved species can be simulated in BIOMOC, ground water flow must be modeled. A two-dimensional (2-D) finite-difference methodology is used for this step that allows the modeler to account for stresses on the ground water system such as pumping from wells or recharge from a surface water source. The flow system can be in a transient or steady state. The finite-difference technique requires that the area being modeled be divided into a grid of rectangles referred to as blocks or cells. Output from the flow model consists of a matrix of hydraulic heads, one for each cell during each model time step. Boundary conditions available in the model include prescribed hydraulic heads and prescribed inflows or outflows (Konikow and Bredehoeft 1978).

The transport portion of the original MOC code solves for chemical concentrations in two separate steps. First, the migration of chemicals due to advection (i.e., migration due to the average linear velocity of ground water) is simulated using a particle-tracking method (Konikow and Bredehoeft 1978). The average linear velocities that govern particle movement are derived from the flow model and an effective porosity that is assigned to the modeled aquifer. During a model time step, each particle in the model domain is assumed to have a concentration associated with it as it is advected from one location to another within the finite-difference grid. Bookkeeping techniques used in the code keep track of the number of particles in the individual grid blocks at any given time. A linear, equilibrium partitioning algorithm is available in this portion of the model to account for the retarded movement of particles used to represent dissolved constituents that sorb to aquifer materials.

The second transport calculation in the MOC simulator accounts for the effects of mechanical dispersion and chemical sources and sinks on the concentrations associated with particles after

they have been moved. This latter step is accomplished using an explicit finite-difference technique (Konikow and Bredehoeft 1978).

In BIOMOC, additional transport calculations are necessary to account for the effects of biodegradation reactions on particle concentrations (Essaid and Bekins 1997). This part of the model also accounts for the growth of the bacteria that mediates these reactions, resulting in computed biomass (bacteria) concentrations at the end of each time step. The algorithms applied in BIOMOC to account for biotransformation of chemical reactants and associated growth of biomass populations (bacterial cells) are those developed by Kindred and Celia (1989). Biotransformation can be simulated using either a multiple Monod or a minimum Monod formulation (Essaid and Bekins 1997). The former is used in this study.

A DOS version of BIOMOC is available to the public through the USGS Internet site http://water.usgs.gov/software/. For this investigation, USGS provided the authors with an alpha version of a graphical user interface (GUI) for the code. In addition to facilitating the input of model parameters, the GUI provided a means for creating snapshot map views of computed concentrations of chemical reactants, including organic acid, natural electron acceptors, and chlorinated ethenes.

4.2 Governing Equations

Ground water flow is simulated in BIOMOC with a numerical approximation of the equation

$$S\frac{\partial h}{\partial t} = \frac{\partial}{\partial x_j}\left(bK_{jk}\frac{\partial h}{\partial x_k}\right) - W \qquad \text{j,k=1,2} \qquad \textbf{(1)}$$

where:
- h = hydraulic head (length),
- S = aquifer storativity (dimensionless),
- t = time (time),
- x_j, x_k = distance in the j and k directions, respectively (length),
- b = saturated thickness of the aquifer (length),
- $\frac{\partial h}{\partial x_k}$ = hydraulic gradient in the k direction (dimensionless),
- K_{jk} = aquifer hydraulic conductivity determining the flow in the j direction due to a hydraulic gradient in the k direction (length/time), and
- W = source or sink fluid flux expressed as a volumetric flow per unit area (length/time).

The solution of Equation (1) produces a set of ground water hydraulic heads that can vary in both space and time. At any given time and location, the computed heads are used to calculate average linear ground water velocity in the j direction (v_j), as given by

$$v_j = -\frac{K_{jk}}{n_e}\frac{\partial h}{\partial x_k} \qquad \textbf{(2)}$$

where: n_e = effective porosity of the aquifer (dimensionless), and

$\frac{\partial h}{\partial x_k}$ = the hydraulic gradient of ground water in the aquifer (dimensionless).

Dissolved species transport is simulated in BIOMOC by accounting for advection, dispersion, sorption on porous medium solids, and chemical reactions in accordance with the equation

$$R_i \frac{\partial C_i}{\partial t} = \frac{1}{b}\frac{\partial}{\partial x_j}\left(bD_{jk}\frac{\partial C}{\partial x_k}\right) - v_j \frac{\partial}{\partial x_j} C_i + \frac{W\left(C_i - C_i^{''}\right)}{(n_e b)} - R_i \lambda_i C_i - B_i \qquad \text{j,k=1,2} \qquad \textbf{(3)}$$

where: C_i = dissolved concentration of the ith chemical constituent (mass/volume),
R_i = retardation factor for the ith constituent (dimensionless),
b = the thickness of the aquifer (length),
D_{jk} = the dispersion coefficient tensor (length^2/time),
$C_i^{''}$ = the concentration of the ith solute in a water source (i.e., water added to the ground water system) (mass/volume),
= the first-order decay constant for the ith constituent (1/time), and
B_i = the biodegradation reaction rate term, representing the uptake of the ith constituent due to biologically-mediated reactions (mass/volume/time).

This equation is solved for every constituent included in a BIOMOC simulation.

Advective transport (i.e., transport due to the average linear ground water velocity) in the BIOMOC code is simulated using the previously mentioned particle-tracking algorithm originally developed by Konikow and Bredehoeft (1978). To account for the fact that the migration of some dissolved constituents can be retarded (Freeze and Cherry 1979) due to their sorption on porous medium materials, the average linear velocity of particles associated with these constituents are slowed in proportion to a dimensionless number known as the retardation factor

$$R_i = 1 + \frac{\rho_b K_{d_i}}{n_e} \qquad \textbf{(4)}$$

where: ρ_b = dry bulk density of the aquifer materials (mass/volume), and
K_{d_i} = soil-water distribution coefficient for the ith constituent (volume/mass).

The effects of hydrodynamic dispersion (i.e., mixing) on the transport of all dissolved, mobile chemicals in the modeled ground water system are handled using a set of hydrodynamic dispersion coefficients D_{jk}, each of which is assumed equal to the product of average linear ground water velocity and a representative dispersivity (Freeze and Cherry 1979). In a 2-D flow system, this formulation requires the input of both a longitudinal and a transverse dispersivity. BIOMOC does not explicitly account for the molecular diffusion component of hydrodynamic dispersion; thus, BIOMOC cannot be used to assess the purportedly large potential of lactic acid produced by HRC to spread via diffusion (Regenesis 2003d) such that reductive dechlorination is widespread.

4.3 Biodegradation Kinetics

The biodegradation term in Equation (3) is handled using a variation of Monod kinetics (Monod 1949) that allows for both the uptake of biodegradable substrate and the growth of bacteria that gain energy from the biodegradation process. For the purposes of the Building 100 pilot tests, a multiple Monod formulation is applied wherein the biodegradation reaction is controlled by the concentration of each of the substances that affect the reaction (Essaid and Bekins 1997; Watson et al. 2003):

$$\mu^n = \mu^n_{\max}\left\{\left(\frac{C_S}{K_{M_S}+C_S}\right)\left(\frac{C_{TEA}}{K_{M_TEA}+C_{TEA}}\right)\left(\frac{C_I}{K_I+C_I}\right)\right\}\frac{X^n_k}{I_b} \qquad \textbf{(5)}$$

where:
- μ^n = the uptake rate of the organic substrate (e.g., acetate and dissolved hydrogen) (denoted with an s) by the nth biodegradation process (mass/volume/time),
- $\mu^n_{\max}$ = the maximum asymptotic specific uptake rate of the substrate (acetate and hydrogen) (1/time),
- C_s = the dissolved concentration of the substrate (mass/volume),
- K_{M_S} = the half-saturation constant for the substrate (acetate or mass/volume),
- C_{TEA} = the concentration of the terminal electron acceptor (TEA) involved in the biodegradation process (mass/volume),
- K_{M_TEA} = the half-saturation constant of the terminal electron acceptor (mass/volume),
- C_I = the concentration of a chemical that inhibits the reaction between the substrate and the electron acceptor (mass/volume),
- K_I = the inhibition constant of the inhibiting chemical (mass/volume),
- X^n_k = the biomass concentration of microbial (bacterial) population k, responsible for the nth biodegradation process (mass/volume), and
- I_b = the biomass inhibition factor (dimensionless).

The biomass inhibition factor in Equation (5) is defined by:

$$I_b = \frac{k_{biok} + X_k}{k_{biok}} \qquad \textbf{(6)}$$

where:
- k_{biok} = the biomass concentration above which the growth of microbial population k becomes limited (mass/volume), and
- X_k = the biomass concentration of microbial population k (mass/volume).

Inclusion of this inhibition factor allows the model user to prevent unbounded growth of a bacterial population.

It should be noted that Equation (5) calls for the concentration of each electron acceptor to be expressed in units of mass per unit volume of fluid. This applies not only to dissolved reactants

but also to natural electron acceptors in solid form, such as ferric iron or solid-phase manganese. Thus, if the model user chooses to use measured soil concentrations of either of these substances, they must be converted from values that are typically given in terms of mass of chemical per unit mass of soil to units of mass of chemical per unit volume of fluid (water). Similarly, for convenience, the biomass concentration used in both Equations (5) and (6) is expressed in units of mass per unit volume of fluid, even though bacterial populations are rarely reported in such units and all microbial populations are treated as non-dissolved and attached to aquifer materials in the BIOMOC code.

Though Equation (5) includes only one expression to account for the inhibition of a biotransformation reaction, BIOMOC is actually versatile in this regard in that several inhibiting substances can be taken into account simultaneously. Thus, it is possible to inhibit methanogenesis if significant concentrations of ferric iron and sulfate, for example, are still present in a ground water system as it gradually passes to a more anaerobic state.

A slightly simplified form of the Monod Equation (5) is actually presented in BIOMOC-related literature that so that only the effects of Monod parameters for the organic substrate and a specific TEA can be more closely examined, rather than focusing all possible inhibition processes. This is accomplished by invoking a dimensionless term that is referred to as the noncompetitive inhibition factor I_{nc}:

$$I_{nc} = \frac{K_I + C_I}{C_I} \tag{7}$$

where all terms on this equation's right-hand-side are as defined earlier. This term is given the "non-competitive" label because the constituent(s) inhibiting the biotransformation process is not an additional organic substrate (e.g., an organic contaminant like toluene) competing with the primary substrate (i.e., acetic acids or dissolved H_2) for chemicals to react with.

Incorporating the above-given expression for I_{nc} in Equation (5) produces:

$$\mu^n = \frac{\mu^n_{\max}}{I_{nc}} \left\{ \left(\frac{C_S}{K_{M_S} + C_S} \right) \left(\frac{C_{TEA}}{K_{M_TEA} + C_{TEA}} \right) \right\} \frac{X_k^n}{I_b} \tag{8}$$

Equation (8) applies to a specific form of bacteria, namely microbial population k. Accordingly, a different form of this equation applies to each biodegradation process. The BIOMOC code accounts for the possibility that multiple degradation processes can simultaneously affect each solute by summing the uptake of the solute (i.e., the removal of the dissolved chemical from solution) resulting from each process:

$$B_i = \sum_{n=1}^{N} \beta_i^n \mu^n \tag{9}$$

where: B_i = the summed uptake of the ith solute for all simultaneously occurring biodegradation processes involving solute (mass/volume/time),

μ^n = the uptake rate of organic substrate by the nth biodegradation process (mass/volume/time),

β_i^n = the uptake coefficient of the ith solute for the nth biodegradation process (mass/mass, or dimensionless), and
N = the total number of biodegradation processes involving the ith solute.

The summed uptake B_i represents the cumulative removal of solute i from ground water as incorporated in the advective-dispersive transport formulation (Equation (3)). When the solute is the primary substrate, β is equal to 1. Otherwise, β is determined by the stoichiometry of the reaction and is equal to the ratio of the mass of solute *i* to that of the primary substrate, i.e.,

$$\beta_i = \frac{\alpha_i \times MW_i}{\alpha_1 \times MW_1} \quad \textbf{(10)}$$

where: α = the stoichiometric coefficient of the solute in the reaction, and
MW = the molecular weight (mass).

The subscript 1 in Equation (10) refers to the primary solute for the reaction and the subscript *i* refers to the solute for which the uptake ratio is being computed. The value of β is negative if the ith solute is produced by the nth biodegradation process and is zero if the solute is not involved in the reaction.

BIOMOC tracks the growth rate of each bacterial population (biomass) that metabolizes substrate. The rate of biomass growth for each population is given by:

$$\frac{dX_k}{dt} = \left(P_k - d_k\right)X_k \quad \textbf{(11)}$$

where: P_k = the specific growth rate for microbial population k (1/time), and
d_k = the specific death rate or maintenance constant (1/time).

Because the effect of nutrients at the Building 100 area on bacterial cell growth in the surficial aquifer is not known at this time, it is assumed in this study that the growth is not limited by nutrient availability. With this assumption, the specific growth rate of population k is simulated in BIOMOC by summing the products of a substrate's specific uptake rate associated with a biodegradation process and the cell-yield coefficient *Y* resulting from that process, i.e.,

$$P_k = \frac{1}{X_k / I_b} \sum_{m=1}^{M} \mu^m Y^m \quad \textbf{(12)}$$

where the superscript denotes the mth biodegradation process out of M possible processes that involve microbial population k. The cell-yield coefficient is a dimensionless parameter that represents the mass of bacteria that is produced per unit mass of substrate. Because it is dimensionless, this coefficient is sometimes expressed as a percentage.

5.0 Model Development and Findings

It was recognized at the outset of this study that simulation of all chemical changes leading up to and resulting in reductive dehalogenation would be challenging. If all possible reactions were accounted for, including the generation of five organic acids and dissolved H_2 and the subsequent reaction of acetic acid and H_2 with electron acceptors, including DCE and VC, as many as 25 or more chemical reactions could be considered. Because of these complexities and limitations regarding the chemical species monitored since the pilot tests began, a more simplified modeling approach was adopted. In particular, the decision was made to not model the generation of each individual acid and H_2 separately, but rather to assume that all of these species could be lumped together and treated as a single reactant that would simply be referred to as "organic acid." Because H_2 concentrations were not measured during the pilot testing, the "observed" mass of this dissolved gas could only be approximated by summing the measured concentrations of the five acids that were monitored (lactate, pyruvate, butyrate, propionate, and acetate). In the model, this lumped measure of organic acid mass was treated as the sole electron donor in the surficial aquifer.

The combining of all measured organic acid concentrations into one model component was similar to an approach adopted by the USGS in its simulations of a site in Minnesota (Essaid et al. 1995). In that study, concentrations of total dissolved organic carbon (TDOC) in an aquifer comprised two components, with the first representing the carbon content of all volatile dissolved compounds, and the second representing all constituents in the non-volatile fraction of TDOC. Each of these lumped measures of carbon content represented a single electron donor source in the USGS model of the Minnesota location.

A distinct advantage of treating summed organic acid concentrations as a measure of electron donor availability was that it made the modeling more tractable. However, there were also disadvantages with this approach. The most obvious disadvantage was that, without measured H_2 concentrations, it was impossible to discern whether the mass represented by the organic acid came close to representing the true electron donor mass. Though it was likely that all acetic acid and H_2 available for uptake by TEAs stemmed from the fermentation of the non-acetate acids (McCarty 1997; Watson et al. 2003), the ratio of mass of H_2 generated to the mass of acid degraded was not unity. This inconsistency in mass exchange meant that the uptake coefficients (β_i) developed for all reactants in the model, as well as parameters affecting Monod kinetics and biomass cell growth, would be different from those that would result from simulating stoichiometric relationships explicitly involving acetic acid and dissolved H_2. In reviewing model findings, therefore, the reader should keep in mind the simplifying assumptions that have been adopted herein.

Though the lumping of all acids and dissolved H_2 into a single reactant had its limitations with regard to analysis of biodegradation at the Building 100 area, it did appear helpful in identifying the relative magnitude of the general types of reactions involved. The model produced for this investigation performs reasonably well in matching observed concentrations at well 0514 of the various solutes assumed to be involved in the degradation reactions (including organic acid) during the first 10 months of the pilot test. Similar models based on this approach have not been developed for the other two test areas; however, the findings from simulating the 0514 area have bearing on the remaining pilot test locations.

5.1 Ground Water Flow

The model of flow and transport in the surficial aquifer at the 0514 area was prepared using a grid containing 80 rows and 100 columns. Each grid block comprised a 0.5-ft by 0.5-ft square, resulting in a domain that was 40 ft wide and 50 ft long. The ground water flow portion of the model was prepared by assuming that (1) ground water migrates directly to the southeast, (2) the flow field is at steady-state, (3) aquifer hydraulic conductivity is spatially uniform, and (4) no ground water sources or sinks occur locally. To produce the flow field, prescribed heads, 10 and 9.85 ft above mean sea level, were invoked along the upgradient and downgradient model boundaries, respectively, resulting in a hydraulic gradient of 0.003.

Figure 6 presents a plot view of the simulated area along with the locations of the injection wells and the single monitoring well for test area 0514. This schematic shows that the assumed ambient direction of ground water flow is skewed from the orientation of injection rows by an angle of about 25 degrees. Specifically, ground water is assumed to flow directly to the southeast, whereas the rows of injection boreholes are oriented more toward the east-southeast.

A uniform hydraulic conductivity of 2 feet per day (ft/day) was assigned to the surficial aquifer in the model, and the aquifer was assumed to be 30 ft thick. Several different effective porosities (n_e) were tested in the model so that average ground water velocities could be computed. Ultimately, as discussed in Section 5.6, a n_e value much smaller than actual aquifer porosity was used to achieve model calibration. The use of this lower value indicated that preferential flow tends to occur in the flow system.

5.2 Advective-Dispersive Transport

In developing the transport portion of the BIOMOC model, it was assumed that neither nitrate nor manganese existed in sufficient quantities in the surficial aquifer to be included in the simulations. The resulting transport model of the 0514 area accounted for concentrations of ten constituents (Table 1), all but one of which were assumed to exist in dissolved form. Given that BIOMOC solves for advective transport via particle tracking, each of the chemical constituents included in the model was assigned a particle type. All non-contaminant dissolved species were assigned particles that were assumed to be non-retarded. Included in this particle class were organic acid, the electron acceptors oxygen (O_2) and sulfate (SO_4), and three chemicals produced by reactions (ferrous iron [(Fe^{2+}], methane [CH_4], and ethene [C_2H_4]). Three contaminants simulated in the model, cis-DCE, trans-DCE, and VC, were assumed to be mildly retarded due to sorption (Table 1). Ferric iron (Fe^{3+}), the single solid constituent included in the model, was considered immobile.

Because the model was developed using an alpha version of a BIOMOC graphical user interface (GUI), some of the boundary conditions and source and sink techniques available in the original MOC code (Konikow and Bredehoeft 1978) were not available for simulating transport in the surficial aquifer. This limitation only affected the manner with which organic acid was allowed to enter the aquifer in the cells containing the injection wells. Instead of invoking prescribed concentrations of organic acid in those cells, the organic acid was added to the flow system using internal boundaries. This required that flows be prescribed along each of the four sides of each internal boundary, and that organic acid concentrations be assigned to those flows. Relatively low prescribed flows were applied at each injection cells so that the uniform flow field remained

virtually undisturbed. The associated boundary organic acid concentrations were adjusted during calibration of the transport model.

Table 1. Chemical Species Included in the BIOMOC Model

Chemical	Function	Assumed Mobility
Organic Acid	Electron Donor	Mobile, Unretarded
Dissolved Oxygen (O_2)	Natural Electron Acceptor	Mobile, Unretarded
Ferric Iron (Fe^{3+})	Natural Electron Acceptor	Solid, Immobile
Ferrous Iron (Fe^{2+})	Transformation Product	Mobile, Unretarded
Sulfate (SO_4)	Natural Electron Acceptor	Mobile, Unretarded
Methane (CH_4)	Transformation Product	Mobile, Unretarded
cis-1,2-dichloroethene (cis-DCE)	Contaminant, Electron Acceptor	Mobile, Mildly Retarded
trans-1,2-dichloroethene (trans-DCE)	Contaminant, Electron Acceptor	Mobile, Mildly Retarded
Vinyl chloride (VC)	Contaminant, Electron Acceptor	Mobile, Mildly Retarded
Ethene (C_2H_4)	Transformation Product	Mobile, Unretarded

Transport properties used in the final model included dispersivities that were largely derived as a result of model calibration. A soil-water partition coefficient (K_d) of 0.10 liters per kilogram (L/kg) was assigned to cis-DCE, trans-DCE and VC, and the dry bulk density of aquifer materials was assumed to be 1.5 kilograms per liter (kg/L). Adopted initial conditions and boundary conditions for all 10 constituents included in the transport portion of the model are listed in Table 2.

Table 2. Initial and Boundary Conditions Adopted in the Transport Portion of the BIOMOC Model

Solute	Initial Concentration (mg/L)	Assigned Concentrations (mg/L)		
		Upgradient Boundary	Downgradient Boundary	Injection Locations
Organic Acid	0.0	0.0	Computed by Model	5000.0
Dissolved Oxygen (O_2)	0.75	0.75	Computed by Model	0.0
Ferric Iron (Fe^{3+})	1.5	0.0	Computed by Model	0.0
Ferrous Iron (Fe^{2+})	2.5	2.5	Computed by Model	0.0
Sulfate (SO_4)	150	150	Computed by Model	0.0
Methane (CH_4)	0.45	0.45	Computed by Model	0.0
cis-1,2-dichloroethene (cis-DCE)	0.04	0.04	Computed by Model	0.0
trans-1,2-dichloroethene (trans-DCE)	0.04	0.04	Computed by Model	0.0
Vinyl chloride (VC)	0.05	0.05	Computed by Model	0.0
Ethene (C_2H_4)	0.0	0.0	Computed by Model	0.0

5.3 Biologically-Mediated Reactions

Seven separate chemical reactions were simulated in the biotransformation portion of the transport model. Inclusion of these reactions resulted in the output of a biodegradation reaction rate term (B_i) for each of the ten constituents included in the model. All of the reactions involved organic acid. Because the various acids potentially resulting from the degradation of HRC (lactate, pyruvate, butyrate, propionate, and acetate) have different chemical formulas, only one of the acids—acetate—was selected to represent their combined influence. And because the

effects of dissolved H_2 on natural and contaminant electron acceptors were presumably accounted for using a single constituent referred to as organic acid, acetate was also selected to represent H_2. This approach to the biological transformation aspects of the modeling meant that the uptake coefficients (β_i) used in the model for secondary substrates would not be truly representative of non-acetate reactions.

The seven reactions simulated in the model are listed in Table 3. Each is given a label describing the type of reaction that is occurring. A listing of the constituents that are (a) consumed during, (b) produced by, or (c) acting to inhibit each of the chemical reactions is presented in Table 4. This latter table also lists the type of bacteria that are assumed to facilitate each reaction. Further discussion of the bacteria types is provided in the following section.

Table 3. Biologically Mediated Reactions Simulated in the BIOMOC Model

1. Aerobic Respiration $CH_3COOH + 2O_2 \rightarrow 2CO_2 + 2H_2O$	
2. Iron Reduction $CH_3COOH + 3.2FeOOH + 4.8H^+ \rightarrow 0.8CO_3^{2-} + 1.2CH_2O_i + 3.2Fe^{2+} + 4.8H_2O$	
3. Sulfate Reduction $CH_3COOH + 0.95SO_4^{2-} \rightarrow 1.9CO_3^{2-} + 0.1CH_2O_s + 0.95HS^- + 2.85H^+$	
4. Methane Production $CH_3COOH + 0.6H_2O \rightarrow 0.6CO_3^{2-} + 0.8CH_2O_m + 0.6CH_4 + 1.2H^+$	
5. cis-DCE Dechlorination $C_2H_2Cl_2 + CH_3COOH + 4H_2O \rightarrow C_2H_3Cl + 2HCO_3^- + 3H^+ + 3H_2 + Cl^-$	
6. trans-DCE Dechlorination $C_2H_2Cl_2 + CH_3COOH + 4H_2O \rightarrow C_2H_3Cl + 2HCO_3^- + 3H^+ + 3H_2 + Cl^-$	
7. Vinyl Chloride Dechlorination $C_2H_3Cl + CH_3COOH + 4H_2O \rightarrow C_2H_4 + 2HCO_3^- + 4H^+ + 2H_2 + Cl^-$	
CH_3COOH = acetate (used to represent organic acids and dissolved hydrogen) O_2 = dissolved oxygen CO_2 = carbon dioxide $FeOOH$ = iron (ferric) hydroxide H^+ = hydrogen ion CO_3^{2-} = carbonate ion CH_2O_i , CH_2O_s , CH_2O_m = general representations of iron-reducing, sulfate-reducing, and methanogenic biomasses, respectively	Fe^{2+} = ferrous iron ion SO_4^{2-} = sulfate ion HS^- = hydrogen sulfide ion CH_4 = dissolved methane $C_2H_2Cl_2$ = cis-DCE, trans-DCE C_2H_3Cl = vinyl chloride HCO_3^- = bicarbonate ion H_2 = dissolved hydrogen Cl^- = chloride ion C_2H_4 = ethene

Reactions 2 through 4 in Table 3 were taken from information presented by Watson et al. (2003) regarding a microcosm study of the Monod kinetics associated with uptake of natural electron acceptors by acetic acid and H_2. The first reaction (aerobic respiration) was developed separately using stoichiometric principles.

Table 4. Biodegradation Processes, the Solutes Involved in Each Process, and the Microbial Population Responsible for Each Process in the Area 0514 Simulation

Reaction	Organic Acid	Dissolved Oxygen, O_2	Ferric Iron, Fe^{3+}	Ferrous Iron, Fe^{2+}	Sulfate, SO_4	cis-DCE	trans-DCE	Vinyl Chloride, VC	Methane, CH_4	Ethene, C_2H_4	Microbe
Aerobic Respiration	C	C									Aerobes
Iron Reduction	C	I	C	P							Fe reducers
Sulfate Reduction	C	I	I		C						SO_4 reducers
Methane Production	C	I			I				P		Methanogens
cis-DCE Dechlorination	C	I			I	C		P			Dechlorinators
trans-DCE Dechlorination	C	I			I		C	P			Dechlorinators
VC Dechlorination	C	I			I			C		P	Dechlorinators

C = consumed
P = produced
I = noncompetitively inhibiting

Reactions 5 through 7 in Table 3 were derived by combining reductive dechlorination reactions presented in Dolfing et al. (2000), wherein H_2 is the electron donor, with H_2-releasing reactions involving the uptake of acetate (e.g., He et al. 2002). Implicit in the application of these equations was that a dechlorinating bacterial population would be competing with other populations, such as sulfate-reducing and methanogenic organisms, for electrons (Smatlak et al. 1996).

From a stoichiometric perspective, the two biologically-mediated reactions for DCE isomers (cis-DCE and trans-DCE, Reactions 5 and 6) are identical. However, these reactions are considered separately in the model because different Monod parameters are adopted for each. Table 5 lists uptake coefficients for each reaction as calculated per Equation (10).

Table 5. Uptake Coefficients Used in the BIOMOC Model of the Area 0514 Pilot Test

Reaction	β_{Acid}	β_{O2}	β_{Fe3+}	β_{Fe2+}	β_{SO4}	β_{CH4}	$\beta_{cis\text{-}DCE}$	$\beta_{trans\text{-}DCE}$	β_{VC}	β_{C2H4}
Aerobic Respiration	1	1.1	0	0	0	0	0	0	0	0
Iron Reduction	1	0	4.7	-3.0	0	0	0	0	0	0
Sulfate Reduction	1	0	0	0	1.6	0	0	0	0	0
Methane Production	1	0	0	0	0	-0.16	0	0	0	0
cis-DCE Dechlorination	1	0	0	0	0	0	1.6	0	-0.6	0
trans-DCE Dechlorination	1	0	0	0	0	0	0	1.6	-0.6	0
VC Dechlorination	1	0	0	0	0	0	0	0	1.04	-0.45

The reader can develop some idea regarding the relative effects of using acetate alone to represent all HRC-derived acids and dissolved H_2 in pertinent reactions by examining the molecular weights (MW) of these constituents with that of acetate. Acetate has a MW of about 58 grams, which is less than the MW of each of the acids lactate, pyruvate, butyrate, and propionate. In contrast, acetate's MW is much greater than that of H_2 (MW $\approx$ 2). Thus the use of acetate's MW in Equation (10) to compute the uptake coefficient (β_i) for a secondary solute in a reaction produces a notably different value than that resulting from using H_2 as the primary substrate. Nevertheless, the model results stemming from the use of acetate in lieu of H_2 are believed to be somewhat representative of biotransformation processes occurring in the surficial aquifer.

5.4 Simulated Bacterial Populations

As shown in Table 4, five general types of bacteria are assumed to be facilitating the seven chemical reactions included in the model. The exact species comprising four of the types—aerobes, iron reducers, sulfate reducers, and methanogens—are not specifically identified in this study. Rather, they are simply assumed to be present in the surficial aquifer without describing their taxonomic composition.

The final type of microbial population used in the model is called a dechlorinator. The exact identity of this organism is unclear; however, it is assumed herein that it comprises a strain (or

possibly strains) of *dehalococcoides* organisms that are essential to the dehalogenation of DCE isomers and VC (see, for example, Chapelle et al. 2003; Major et al. 2003).

5.5 Model Testing and Calibration

Before conducting calibration runs with the model, several simulations were made to preliminarily assess the sensitivity of predicted concentrations of all 10 model constituents to a variety of model inputs. Initial testing focused on flow model parameters and model inputs that influence particle velocity in the surficial aquifer. This was followed by assessments of the influence of transport model parameters on constituent distributions, particularly the distribution of organic acid. Final model calibration was achieved mostly by adjusting the numerous Monod parameters that have an effect on computed degradation and production rates. Included in this latter parameter category were variables that influence microbial growth, such as initial concentrations of the five types of bacteria assumed to be present at the site.

5.5.1 Model Sensitivity to Parameters Affecting Ground Water Velocity

It was known at the outset of the modeling that effective porosity (n_e) of the surficial aquifer plays a significant role in controlling organic acid concentrations as well as the concentrations of all remaining constituents whose values change in the presence of acetic acid and H_2. As indicated by Equation (2), the average linear ground water velocity (v_i) increases as n_e decreases. And with increasing velocity, the average travel time for a molecule of water traveling between an HRC-injection location and the closest downgradient monitoring well will decrease. Monitoring of organic acid concentrations in the 0514 area during the pilot testing did indicate that the that travel time between the closest upgradient injection location and well 0514 was shorter than that predicted by assuming that surficial aquifer's effective porosity is close in value to aquifer's full porosity. Full porosity is likely to range between 0.30 and 0.35.

Initial estimates of model values of n_e were derived using the Darcy's Law, as expressed in Equation (2). Using an average hydraulic conductivity of 2 ft/day, an aquifer hydraulic gradient of 0.003, and an initial n_e of 0.30, which resulted in an average ground water velocity of 0.02 ft/day. Dividing the distance between well 0514 and the closest upgradient injection borehole (~5 ft) by this velocity produced an average ground water travel time of 250 days. However, as discussed in Section 3.2.2, organic acids began showing up in well 0514 within 3 months (90 days) of starting the pilot test. Thus it appears that the average linear ground water velocity and hence effective porosity of the aquifer are considerably smaller than expected. This observation holds true even if other factors that could increase ground water velocity are taken into account. For example, longitudinal dispersion has the potential to drive the leading edge of the organic acid plume ahead of the average linear velocity, but certainly not to the extent observed. Similarly, even if the average hydraulic conductivity of the aquifer was assumed to be twice the adopted value of 2 ft/day, and all other Darcy Law parameters remained at their originally assumed values, organic acid would still not be expected at well 0514 until after a period of 6 months or more.

Preliminary runs with the model aimed at matching observed concentrations of organic acid and all constituents potentially affected by reactions that include acetic acid and H_2 indicated that effective porosity of the aquifer is probably no greater than 0.15, and more than likely hovers around values ranging from 0.05 to 0.10. An important implication of these observations was that much of the area simulated in the model as being affected by the presence of organic acid

was probably not being affected at all. That is, the capacity of organic acid to penetrate portions of the aquifer volume not represented by the effective porosity was likely limited to very slow rates, such as those associated with aqueous-phase diffusion in porous media.

5.5.2 Effects of Dispersivity

Several different values of longitudinal and transverse horizontal dispersivity were tested during initial simulations with the model. As is often the case, the potential for predicted plumes of injectate products (in this case HRC-derived acids) to move upgradient of injection locations increased substantially with increasing dispersivity values. Frequently, the use of relatively large aquifer dispersivities resulted in temporal plots of concentration that faired poorly in matching observed constituent concentrations. Ultimately, model calibration was achieved using longitudinal dispersivity values that fell into a range that represented 1 to 10 percent of the transport lengths affected by the pilot test in the 0514 area. This percentage range has been shown to be applicable to aquifers affected by scale-dependent dispersion (e.g., Gelhar et al. 1985).

5.5.3 Model Sensitivity to Monod Parameters

Aside from effective porosity, the parameters that appeared to have the greatest influence on computed concentrations during preliminary model simulations were those that associated with Monod kinetics, i.e., parameters incorporated in Equation (8). Included in this category were variables that characterize biomass growth rates, as described by Equations (11) and (12).

Where possible, initial estimates of maximum degradation rates ($\mu^{n}_{\max}$) and half-saturation constants (K_{M_S}, K_{M_TEA}) were drawn from previous studies aimed either at (1) quantifying the reactions of electron donors acetate and hydrogen with various natural electron acceptors (e.g., Watson et al., 2003), or (2) describing the anaerobic biotransformation of chloroethenes (e.g., Essaid and Bekins 1997; Skeen et al. 1996). However, no attempt was made to rigorously restrict values of these Monod parameters to narrow ranges encompassing their initially estimated values. There was little impetus for doing so given that the mass quantities associated with modeled reactions, all of which involved a lumped measure of organic acid concentration rather than individual concentrations for acetate and H_2, were inherently different from those that would result from actual reactions involving the electron donors acetate and H_2 and a variety of electron acceptors. Consequently, maximum degradation rates and half-saturation constants for both organic acid and the TEAs included in the modeled reactions (Table 3) were ultimately treated as calibration parameters. A disadvantage of this approach was that it was difficult to determine whether final model estimates of the Monod parameters were grounded in site-specific data. Accordingly, it is likely that better estimates of degradation rates and half-saturation constants could be derived from ancillary investigations based on microscosm testing.

For lack of site-specific data or microcosm study findings, model parameters affecting microbial growth were also largely treated as model calibration parameters. Reasonable values of such parameters as initial microbial population concentrations and cell yields were first drawn from data presented in previous modeling studies (e.g., Essaid et al. 1995; Watson et al. 2003) and subsequently adjusted to reflect assumed conditions in the Building 100 area. One of the assumptions made was that iron-reducing bacteria existed at relatively high concentrations in the surficial aquifer prior to the pilot test due to ambient, yet slow, reductive dechlorination of DCE isomers.

Initial testing of non-competitive inhibition constants (K_I) in the model demonstrated that they effectively delayed the dechlorination of cis-DCE and VC until sulfate-reduction and methanogenic microbial processes became fully active. Without knowledge of the exact processes that effect inhibition of dechlorination in surficial aquifer materials, K_I values were largely treated as simple model calibration parameters.

5.6 Final Model Parameters

Numerous runs were made with the BIOMOC simulator until arriving at a set of Monod and microbial growth parameters that resulted in a reasonable match of observed trends in constituent concentrations at monitor well 0514. Effective porosity (n_e), which had profound effects on computed concentrations at the well, was assigned a final value of 0.10 (10 percent). Assuming actual aquifer porosity is 0.30, this n_e value represented only about a third of the total pore space occupied by ground water. The remaining two-thirds was assumed to comprise aquifer zones characterized by lower hydraulic conductivities than the K_{jk} [Equation (1)] value of 2 ft/day applied uniformly throughout the model.

As mentioned in Section 3.2.2, several lines of evidence from the first 10 months of the pilot testing indicated that HRC-derived acids, and possibly dissolved H_2, are no longer being delivered to the well 0514 location. This in turn suggested that generation of lactic acid from biological breakdown of HRC at the upgradient injection borehole closest to this well stopped occurring at some point during the period covered by this modeling study. In an effort to match the summed concentration of organic acid at well 0514, the acid source at each injection location in the test area was terminated in the model at some point during the simulation period. The final calibrated model assumes that HRC becomes depleted 3.5 months after its injection.

Longitudinal dispersivity in the final model was assigned a value of 0.5 ft. This length represented 10 percent of the distance separating well 0514 from the closest HRC injection location (~ 5 ft) and approximately 2 percent of the distance a molecule would travel on average during the course of year given the adopted model parameters. Transverse horizontal dispersivity was assigned a value of 0.05 ft.

The final model inputs for Monod parameters and variables affecting microbial growth are listed in Table 6. Further discussion of some of these parameter values is provided in the following section that presents comparisons between observed and model-computed concentrations.

5.7 BIOMOC Model Results

The results of the final calibrated BIOMOC model of the pilot test are illustrated using both temporal plots of model-computed and observed concentrations of constituents at well 0514 and map views of computed constituent concentrations at selected times. The temporal plots provide some measure of the model's ability to simulate the cumulative effects of biotransformation processes at a single location. Though the mapped views of predicted concentration distributions cannot be compared to observed equivalents, they do give the reader a perception of the aquifer volume potentially affected by HRC injection. They can also be used to roughly project future effects of the pilot test in the 0514 area.

Table 6. Monod and Biomass Growth Parameters Used in the Calibrated BIOMOC Model

Model Constituent, *i*	**Maximum Degradation Rate,** $\mu_{\max}^{n}$	**Primary Substrate Half-Saturation Constant,** K_{M_S}	**Terminal Electron Acceptor Half-Saturation Constant,** K_{M_TEA}	**Non-Competitive Inhibition Constant,** K_I	**Initial Biomass Concentration,** X_k^n	**Cell Yield Coefficient,** Y^m	**Specific Death Rate,** d_k	**Biomass Inhibition Constant,** k_{biok}
	(sec^{-1})	(mg/L)	(mg/L)	(mg/L)	(mg/L)	(percent)	(sec^{-1})	(mg/L)
Reaction (n) = Aerobic Respiration, Biomass (k) = Aerobes								
Organic Acid	1×10^{-3}	3.0			1×10^{-4}	30	2.3×10^{-7}	0.1
Oxygen			2.0					
Reaction (n) = Iron Reduction, Biomass (k) = Fe Reducers								
Organic Acid	1×10^{-3}	3.0			0.1	30	2.3×10^{-7}	1.0
Oxygen				0.75				
Ferric Iron			0.75					
Reaction (n) = Sulfate Reduction, Biomass (k) = Sulfate Reducers								
Organic Acid	1×10^{4}	6.0			1×10^{-3}	30	2.3×10^{-7}	0.25
Ferric Iron				1.0				
Oxygen				0.75				
Sulfate			6.0					
Reaction (n) = Methane Production, Biomass (k) =Methanogens								
Organic Acid	7×10^{-5}	30.0			5×10^{-6}	30	2.3×10^{-7}	0.1
Oxygen				0.75				
Sulfate				140.0				
Reaction (n) = cis-DCE Dechlorination, Biomass (k) = Dechlorinators								
Organic Acid	2.5×10^{-4}	3.0			5×10^{-4}	10	0.0	0.5
Oxygen				0.75				
Sulfate				140.0				
cis-DCE			10.0					
Reaction (n) = trans-DCE Dechlorination, Biomass (k) =Dechlorinators								
Organic Acid	1×10^{-6}	6.0			5×10^{-4}	10	0.0	0.5
Oxygen				0.75				
Sulfate				140.0				
trans-DCE			10.0					
Reaction (n) = VC Dechlorination, Biomass (k) = Dechlorinators								
Organic Acid	2.5×10^{-4}	3.0			5×10^{-4}	10	0.0	0.5
Oxygen				0.75				
Sulfate				140.0				
VC			10.0					

5.7.1 Results During the Initial Ten Months of Testing

Organic Acid

One of the main objectives of model calibration was to match the sum of observed concentrations of organic acids at well 0514 shown in Figure 5. As illustrated in Figure 7, the

model performs reasonably well in achieving this goal. The computed organic acid concentration, like observed values, peaks at about 6 to 7 months after injection of HRC, and drops off relatively rapidly thereafter. The peak observed concentration of organic acid is about 190 mg/L, and the model-generated equivalent is approximately 230 mg/L. Both observed and computed concentrations of organic acid register zero values 10 months after injection.

Despite the relatively good fit between computed and observed organic acid concentrations, noticeable time lags exist between the plotted curves for each (Figure 7), both during the rise in acid concentration and its decline. Observed acid concentrations begin to significantly increase about 2 months after HRC injection, whereas model-generated values of acid level do not occur until about 2 months later. Part of this discrepancy might be attributed to dispersion effects in that a larger longitudinal dispersivity than the 0.5-ft value used in the model might have caused computed organic acid concentrations to increase earlier than is indicated in Figure 7. However, an equally plausible explanation for the apparent time lag between observed and computed acid increases is that the effective porosity of the aquifer is even lower than the n_e of 0.10 used in the calibrated model.

The apparent time lag between observed and computed concentrations during the recession stage of the acid levels at well 0514 is about one-half month. This time lag is considered somewhat useful for the model simulation because it makes available additional electron donor mass that potentially represents dissolved H_2 concentrations in the aquifer. Obviously, however, it is impossible, without measured H_2 concentrations, to assess whether the computed acid concentrations compensate adequately for this donor capability.

Figures 8 and 9 present areal views of computed organic acid concentrations in the 0514 test area at 2 months and 6.5 months, respectively, after the time of injection. The first of these figures suggests that, during initial stages of the pilot test, the summed concentration of all organic acids in the immediate vicinity of the injection boreholes reached values exceeding 900 mg/L, and that acid concentrations elsewhere in the test area remained quite low. At the time represented by the second plot, shortly after the computed acid concentration peaks at well 0514, the acid plume has begun to move beyond this well, and no additional upgradient acid sources are delivering electron donors to it.

Dissolved Oxygen

A graph comparing computed and observed oxygen levels at well 0514 (Figure 10) shows that this constituent, whose initial values are low to begin with (0.75 mg/L), drop very quickly during the first 1 to 2 months of the test, and begin the process of recovering to pre-test concentration magnitudes about 8 to 9 months into the test. As in the case of organic acid, a time lag is apparent between observed and computed O_2 concentrations, during both the initial and later stages of the test. This time lag would be less than observed if average linear ground water velocity in the model were increased by decreasing the assumed effective porosity (n_e) to a value lower than 0.10.

It is interesting to note that the model computes O_2 concentrations of zero during the period that organic acid is present at well 0514, whereas observed concentrations tend to hover around a value of 0.1 to 0.2 mg/L at this time. This result suggests that the aquifer is prevented from being driven completely anoxic by a yet-to-be identified mechanism. However, it might also reflect the sensitivity of the instrument used to measure DO levels.

Dissolved Iron

Model-predicted levels of dissolved ferrous iron (Fe^{2+}) at well 0514 are vaguely similar to observed equivalents (Figure 11) only during the first 1 to 1.5 months of the test. Thereafter, observed Fe^{2+} levels drop rapidly to values that are about five times less than the starting dissolved iron concentration (~ 2.5 mg/L). In contrast, computed ferrous iron concentrations decline at a very slow pace from their peak value (~ 3.6 mg/L), which is predicted to occur about 2 months after the test start. This very obvious discrepancy is most likely explained by an additional chemical reaction or multiple reactions that lead to the precipitation of Fe^{2+} in solid form. Previous studies have attempted to explain the nature of such precipitation at sites contaminated by organic contaminants (e.g., Tuccillo et al. 1999). It is probable that the Fe precipitate in the 0514 area, if it does exist, stems from reactions involving chemical reduction of iron and sulfate, both of which occur in response to the presence of acetate and dissolved hydrogen in the test area.

Kennedy et al. (1998; undated) reports that the dissolved Fe^{2+} produced by the reduction of mineral-form iron shows a tendency to precipitate in any of several forms, including iron sulfides (FeS or FeS_2). The associated iron chemistry in such areas can be complex, with the potential existing for some iron sulfides to form from relatively slow reduction of solid Fe^{3+} in abiotic reactions set apart from those involving microbially-generated Fe^{2+}. Though the exact explanation for disparities in computed and observed ferric iron concentrations (Figure 11) cannot be explained at this time, further analysis of this issue would help to better quantify the role that iron-reducing bacteria play in affecting electron donors that contribute to dechlorination of DCE and VC.

Assay work on soil samples collected from the surficial aquifer at the Building 100 area indicated that the amount of bioavailable Fe^{3+} in this location was quite limited (CDM 2003). However, given the relatively strong response of dissolved Fe^{2+} to the appearance of organic acid at well 0514, it would be premature at this time to conclude that iron reduction plays a minor role in the biotransformation processes that lead up to reductive dechlorination of DCE and VC. This observation is particularly true given that the bioassay technique used by CDM to quantify the amount of solid phase iron that can be reduced during biodegradation is only one of several diverse methods that can be applied for such a determination (e.g., Heron et al. 1994; Kennedy et al. 1998; Tucillo et al. 1999), and that each of these methods can easily produce noticeably different estimates of bioavailable iron. Accordingly, further investigation of iron chemistry in the surficial aquifer in response to the addition of amendments intended to bring about chemically reducing conditions and eventual dechlorination would appear warranted.

Sulfate

The temporal behavior of observed and computed sulfate (SO_4) concentrations at well 0514, presented in Figure 12, indicates that the model performs well in matching observed decreases in SO_4 levels during the first 3 months of the test study, but lags behind when predicting the eventual increase in the concentration of this constituent during later months. It is likely that the temporal lag in this case might have been minimized had the model been developed using an effective porosity lower than 0.10. However, the possibility that the discrepancy between observed and predicted SO_4 levels between months 6 and 10 of the test is due to as yet undefined chemical reactions involving both iron and sulfate cannot be discounted. Regardless of the

factors contributing to the results shown in Figure 12, it is clear that the sulfate-reducing microbial activity that probably led to SO_4 reductions during the first few months of the test has since subsided greatly.

An areal depiction of computed SO_4 concentrations in the 0514 area after 2 months of testing (Figure 13) indicates that areas where this TEA has been depleted are limited to the locales affected by the presence of organic acid at this time (Figure 8). Areas of reduced sulfate concentration at 6.5 months into the study (Figure 14) occur in the organic acid at this time (Figure 9). However, Figure 14 also implies that the area within the model domain affected by sulfate reduction is larger than that affected by organic acid presence, which in turn suggests that electron donor concentrations need not be extremely large to bring about methanogenesis and reductive dechlorination.

Methane

A temporal plot of methane concentrations at well 0514 (Figure 15) shows that the model captures the observed rapid increase in methanogenic activity between the third and fifth months of the test as well as a gradual drop in methane (CH_4) concentrations between the sixth and tenth months. In addition the predicted peak CH_4 concentration (~ 10 mg/L) is close in magnitude to the observed peak of about 11 mg/L. In contrast to the temporal plots for O_2 and SO_4 (Figures 10 and 12, respectively), predicted changes in CH_4 levels during the first half of the ten-month observation period do not lag behind observed changes. A slight lag in predicted concentrations for CH_4 behind observed values (Figure 15) during the recession part of the concentration plot is not as significant as that observed for sulfate (Figure 12).

A map view of model-generated methane concentrations at 6.5 months after injection (Figure 16) suggests that CH_4 plumes stemming from HRC injection cover only a relatively small portion of the 0514 test area. This in turn implies that the methanogenic conditions thought to be most conducive to reductive dechlorination of DCE isomers and VC (Bradley 2000) are not as widespread as those attributed to sulfate reduction in the model (Figure 14).

cis-DCE

As mentioned in Section 3.2.2, cis-DCE concentrations at well 0514 have shown moderate decreases during the pilot testing, which are presumably the result of HRC injection. However, cis-DCE levels at this well have not dropped below the MCL for this constituent (0.07 mg/L). The behavior of cis-DCE during the last two sampling events assessed in this study is of interest because it shows a decrease in the rate of contaminant loss, but recovery of cis-DCE concentrations in concert with declines in measured organic acid concentration, as observed with dissolved O_2 and SO_4, are not apparent. A possible cause of the relatively constant late-time concentrations is the presence of electron donor in the form of dissolved H_2. If H_2 is persisting locally at relatively significant levels, it might be facilitating reductive dechlorination of cis-DCE without being substantially consumed by methanogens or sulfate-reducing bacteria.

Given the behavior of cis-DCE during the test, the decision was made to simulate its gradual decrease over the first 10 months of testing using Monod parameters that approximate a first-order degradation process during part of that time. This was accomplished by using a relatively

small value of maximum degradation rate for the cis-DCE dechlorination reaction ($\mu^{n}_{\max}$ = 2.5 × 10^{-4} sec^{-1}) and a large half-saturation constant for cis-DCE (K_{M_TEA} = 10 mg/L).

The resulting computed cis-DCE concentrations at well 0514 (Figure 17) show a gradual decline that begins about 3 months into the pilot test and levels out about 9 months after HRC injection. In contrast, observed cis-DCE levels show an increase after 1 month of testing, followed by a gradual decrease in concentration until the fifth month of the test, after which concentrations hover about a value of about 0.01 mg/L. The apparent discrepancies between model-predicted cis-DCE concentrations and observed equivalents highlight a need to better understand the factors leading up to and contributing to cis-DCE dechlorination.

An areal plot of computed cis-DCE levels about 9 months after HRC injection (Figure 18) shows the most significant concentration decreases occurring downgradient of injection locations. The smaller, yet discernible, decreases in predicted cis-DCE concentrations between the areas most affected by injection are probably optimistic because of the first-order degradation approximation used to roughly match concentrations of this constituent at well 0514. This approximation technique, when applied using the multiple Monod formulation in Equation (8), predicts substantial degradation of cis-DCE in the presence of even the smallest of computed organic acid concentrations. It is likely that organic acid concentrations (and hence concentrations of acetate and dissolved H_2) would have to be much larger than predicted by the model to effect dechlorination of cis-DCE in areas lying midway between injection locations.

trans-DCE

Decreases in trans-DCE levels at well 0514, if they have occurred as a result of the pilot testing, were also simulated using Monod parameters that approximated a first-order degradation process (Table 6) during a portion of the first 10 months of the test. The concentration-versus-time graph comparing predicted and observed trans-DCE levels (Figure 19) at the well shows why it is difficult to conclude that degradation of this contaminant is occurring in response to HRC application. The areal plot of computed trans-DCE concentrations nine months after HRC injection (Figure 20) illustrates just what little degradation of this contaminant, if any, would be expected.

Vinyl Chloride

It is difficult to interpret the temporal behavior of observed VC concentrations at well 0514 for the initial 10 months of the pilot test. Observed VC levels decreased during the first 3 months after HRC injection but subsequently increased to a peak value at 5 months into the test (Figure 21). The latter increase in concentration might be attributable to production of VC by cis-DCE degradation that first appeared to occur in earnest during the test's third month (Figure 17), but the prior decline in VC concentration seems to be too early to be explained by reactions with available electron donors. More logically, the VC concentration decreases in the early part of the test might be attributed to natural spatial and temporal variability of measured contaminant concentrations at the site. Regardless of the nature of VC concentration changes during the first half of the test, the observed data do indicate a gradual decline in VC levels during the second half (Figure 21), which is probably the result of chemical changes brought on by HRC application.

Again, because of the apparently complex behavior of observed contaminant levels during the 10 months of testing examined in this study, changes in VC concentration at well 0514 were simulated in the model using Monod parameters (Table 6) that approximated a first-order degradation process over a portion of the initial 10 months. This approach produced VC levels (Figure 21) that began declining about 3 months into the test from an initial concentration of 0.05 mg/L to about 0.03 mg/L at 10 months. Actual VC concentration at well 0514 during the ten-month sampling event was approximately 0.02 mg/L.

Computed VC concentrations over the 0514 test area at 9 months after injection (Figure 22) suggest that the approximate halving of initial VC levels at well 0514 is about the maximum decrease that could be expected at any point at the site during the test. Well 0514 is situated in an area where the effects of HRC injection at two upgradient locations are capable of augmenting each other, thus achieving the greatest amount of dechlorination. In between these locations, however, and midway between injection locations, the potential for dechlorination of VC appears less likely (Figure 22).

Ethene

As illustrated in Figure 23, the model tends to match incipient increases in observed ethene concentrations (from VC degradation) in well 0514 at about 4 months after HRC injection, but over-predicts peak C_2H_4 concentration and delays its occurrence by about two months. Nevertheless, the concentrations predicted by the model for this transformation product fall into the general range of its observed concentrations.

5.7.2 Estimated Concentrations One Year After HRC Injection

Current plans call for monitoring associated with the pilot test to proceed for up to a year or more after the HRC injection on March 11, 2003. Consequently, the total simulation time covered by the BIOMOC model was 1 year. This section addresses resulting predictions for some of the ten model constituents between the tenth and twelfth months of the test to help facilitate interpretation of concentrations recorded during a seventh sampling event.

Because the model has been developed under the assumption that all reactions are, to some degree or another, dependent on the presence of organic acid, and the model has indicated that organic acid concentrations at well 0514 have declined to non-detectable levels, the model predicts a gradual return to pre-test levels for constituents reflective of reactions involving natural electron acceptors. The same cannot necessarily be said, however, about DCE isomers and VC because of parameters that have been applied to these contaminants in the model to approximate first-order degradation effects.

As shown in Figures 10 and 12, the model predicts that dissolved oxygen and sulfate levels at well 0514 will continue increasing toward pre-test levels between 10 and 12 months after injection. In contrast, the transformation product methane is expected to continue declining in concentration during this period (Figure 15). A model-predicted gradual decline in dissolved Fe^{2+} levels (Figure 11) during this time should not be used to evaluate test results because of the current model's inability to account for the likely precipitation of ferric iron in solids.

The previously discussed temporal plots of cis-DCE and VC concentration (Figures 17 and 21) show that the model is predicting slight increases in the levels of these constituents at well 0514

during the remaining few months of a year-long monitoring period. It should be noted, however, that these predicted increases occur because the computed organic acid concentration at this time is zero, and the model is incapable of accounting for dissolved H_2 in the surficial aquifer that might persist for months after the disappearance of detected organic acid. This persistent H_2, if actually present, might be capable of at least maintaining cis-DCE concentrations at their most recent lows (via reductive dechlorination) if not decreasing their concentrations below observed values at 10 months into the test.

Concentrations of trans-DCE between the tenth and twelfth months of the study are predicted to continue a gradual decrease (Figure 19). The magnitude of this decrease is far less than the range of measured levels of trans-DCE during the test thus far; consequently the model is of little utility at this time for assessing future concentrations of this constituent.

The spatial distribution of computed organic acid concentrations after 1 year of pilot testing in the 0514 area (Figure 24) indicates that the only significant acid levels would be observed in the adjacent to and downgradient of the most-downgradient injection locations. These predicted acid concentrations suggest that little to no potential exists for continued degradation of DCE isomers and VC in the test area. Again, however, the reader is cautioned that such an interpretation is premature because of the model's inability to account for dissolved H_2 concentrations after 1 year of testing.

The influence of model-generated acid concentrations on computed cis-DCE and VC concentrations at 1 year into the test is seen in Figures 25 and 26, respectively. Both areal plots are similar to equivalent map views of these constituents at nine months into the test (Figures 18 and 22) as they suggest that decreasing concentrations of chloroethenes remain pervasive downgradient of injection boreholes. In addition, reductive dechlorination midway between injection locations is still predicted to be active. However, the reader is reminded that these latter results are probably optimistic because they result from the first-order degradation approximations used to simulated cis-DCE and VC, and are not truly reflective of the Monod kinetics associated with chloroethene reduction.

5.8 Summary of BIOMOC Findings

The model of the area 0514 pilot test demonstrates that it is possible to use a ground water transport model containing Monod kinetic algorithms to simulate the effects of enhanced bioremediation of chlorinated ethenes via reductive dechlorination. The model, based on the USGS simulator BIOMOC (Essaid and Bekins 1997), performs reasonably well in matching observed concentrations of selected constituents in a local monitor well over a ten-month period following injection of the amendment HRC, which is designed to promote reductive dechlorination.

Several assumptions were made in developing the model, partly for the purpose of making the model tractable, but also partly out of necessity due to monitoring data limitations. Perhaps the greatest limitation is that concentrations of dissolved hydrogen (H_2), which, along with acetic acid (acetate), is a primary electron donor facilitating eventual reductive dechlorination, have not been measured during the pilot test. As a consequence, the summed concentration of all acids potentially derived from degradation of HRC through a series of fermentation reactions has been used to estimate the total electron donor mass available for biodegradation processes. This simplified approach to the problem results in Monod parameters and constituent uptake

coefficients that are not truly reflective of the parameter values that would result from specifically simulating acetate and dissolved H_2. This shortcoming highlights a need for collecting H_2 concentration data during future implementations of enhanced bioremediation at the STAR Center.

Despite the limitations associated with model simplifications, two distinct conclusions can be drawn regarding constituent transport in the surficial aquifer. First, the effective porosity of the aquifer is apparently much lower than its estimated full porosity, which in turn signifies a tendency toward preferential flow in the subsurface. An effective porosity of 0.10 was used to calibrate the BIOMOC model; however, several lines of evidence drawn from model results suggest that the effective porosity of the local ground water system is even lower than this value. If preferential flow predominates in the surficial aquifer, it is likely that only a portion of the areas simulated as being affected by HRC-derived acids (see map views of computed constituent distributions in the previous section) would have actually been affected. Consequently, less permeable portions of the aquifer that contain chloroethenes in the form of DCE isomers and VC are less likely to have been impacted by the HRC application during the pilot test.

The second distinct conclusion drawn from modeling of the area 0514 test is that iron contained in the surficial aquifer probably takes part in chemical reactions brought on by injection of the HRC amendment. During the modeling, these reactions caused predicted ferrous iron (Fe^{2+}) concentrations to be much larger than observed concentrations. The most likely explanation for this discrepancy is that ferrous iron was abiotically reacting with other system constituents (such as sulfides generated by sulfate-reducing bacteria) to form solids that precipitate out of solution. Though this ancillary reaction, if it occurs, does not directly impact chloroethene degradation, it potentially affects biologically-mediated reactions that must occur before reductive dechlorination can take place. Thus the impetus exists to better understand the iron chemistry of the surficial aquifer when applying bioremediation amendments.

Model simulation of DCE and VC degradation did not lead to insightful conclusions regarding reductive dechlorination of these contaminants in response to HRC treatment. Both cis-DCE and VC concentrations in well 0514 decreased moderately during the test, apparently in response to HRC-derived electron donors in the vicinity of the well. However, it was difficult to discern Monod parameters that effectively described these decreases. This obstacle might have been partially overcome had H_2 concentrations been measured during the test, and H_2 was treated as a separate constituent in the model. It is likely that parameters affecting reductive dechlorination of cis-DCE and VC could be better quantified through microcosm testing.

Relatively mild to moderate decreases in cis-DCE and VC concentrations during the pilot test suggest that currently unknown factors are limiting the reductive dechlorination process. Such a factor might occur in the form of limited availability of nutrients that are integral to the biotransformation processes involved. Because data regarding nutrients at the test site were not available, their effects on biotransformation reactions were not simulated in the model. Algorithms describing the influence of nutrients on the specific growth rate of a microbial population are available in the BIOMOC code (Essaid and Bekins 1997) should the need arise to account for them in the surficial aquifer. It is also possible that the efficacy of dechlorinating bacteria in degrading cis-DCE and VC is being hampered by competition for electron donors by sulfate-reducing or methanogenic bacterial populations (e.g., Fennel et al. 1997; Yang and McCarty 1998).

End of current text

6.0 Conclusions

Computer modeling of an enhanced bioremediation pilot testing in the Building 100 Area at the STAR Center demonstrates that it is possible to approximately simulate the effects of amendment applications to the local surficial aquifer for the purpose of stimulating reductive dechlorination of chloroethene contaminants. Pilot tests were based on the release of HRC (Regenesis 2003a) to the subsurface via several injection boreholes. Modeling of one of the areas included in the tests was performed using the code BIOMOC (Essaid and Bekins 1997), which was developed by the USGS. BIOMOC facilitated the simulation of not only advective-dispersive transport in the local ground water system, but also the fate of ten separate constituents involved in seven different biologically mediated reactions. This represented a marked improvement over a previous modeling effort (DOE 2003b) that was capable of only representing biotransformation in the surficial aquifer in a primitive manner.

Despite the relative success of the BIOMOC modeling effort, several simplifications were adopted in the course of developing the model that tended to hamper some of the study's findings. A particularly limiting assumption made in the model was that concentrations of a significant electron donor capable of driving reductive dechlorination — namely dissolved hydrogen — were not taken into account. This approach was adopted because dissolved hydrogen concentrations were not measured in samples collected from pilot test monitor wells, thus denying the opportunity to use temporal changes in this constituent's mass as a model calibration target. In lieu of simulating dissolved hydrogen concentration, the summed concentration of five organic acids potentially derived from HRC was used to represent the mass of the two electron donors (acetic acid and dissolved hydrogen) that can lead to reductive dechlorination of the contaminants DCE and VC (McCarty 1997).

The model prepared under this investigation simulated ground water flow and transport of several constituents in the vicinity of a pilot test encompassing monitor well 0514. This location was picked because the effects of HRC injection were much more evident here than they were at two additional locations included in the pilot testing. Measured concentrations of several constituents in well 0514 were used to calibrate the model, which was constructed with the intent of accounting for HRC injection at nine separate locations surrounding the well.

Despite the potential shortcomings of the simplified modeling approach adopted for this investigation, several conclusions could be drawn from attempting to simulate transport in the test area associated with well 0514. These conclusions most likely apply to all areas of the local shallow ground water system that are contaminated by chlorinated solvents:

1. The biologically mediated reactions between bioremediation amendments or their transformation products and electron acceptors in the subsurface can be successfully simulated using a transport model that allows for Monod kinetics.

2. Given accurate stoichiometric relationships between HRC-derived acids and dissolved hydrogen, it should be possible to accurately track the mass of acetic acid and hydrogen that is available as electron donor material for all biologically mediated reactions.

3. The transport of HRC transformation products (organic acids, dissolved hydrogen) in the STAR Center surficial aquifer is strongly affected by preferential flow, as model-generated effective porosities appear to be three to five times smaller than actual aquifer porosities.

4. Because of the predominance of preferential flow, it is likely that many aquifer areas lying between HRC injection points are not being impacted by chemicals capable of driving reductive dechlorination of chloroethenes, even if those areas appear to lie directly in the path of natural ground water flow away from the injection locations.

5. Comparison of model simulations with observed dissolved ferrous iron concentrations indicates that iron reduction is a major pre-dechlorination reaction that, along with sulfate reduction, strongly affects the ground water system's ability to reach conditions conducive to dechlorination; however, iron reduction effects are difficult to quantify because abiotic reactions that likely cause precipitation of reduced iron have yet to be fully identified.

6. The longevity of HRC-generated organic acids at HRC injection points appears limited to less than a half-year.

7. As a result of an apparent limit on HRC persistence in the surficial aquifer, the availability of electron donor mass (acetic acid and hydrogen) for reductive dechlorination at any one location in the aquifer is likely limited to a period of somewhere between 0.5 and 1.5 years.

8. Concentrations of the contaminants cis-DCE and VC during the pilot test decreased slightly to moderately in locations affected by HRC transformation products, but did not decrease sufficiently to drive VC levels below the applicable regulatory standards for this contaminant.

9. The apparently slow and incomplete degradation of cis-DCE and VC partially reflect difficulties with identifying the factors contributing to dehalogenation of these compounds, and the Monod kinetics describing their dehalogenation.

10. Possible factors contributing to incomplete dechlorination of cis-DCE and VC include limited nutrient availability and competition for the electron donor dissolved hydrogen between dechlorinating microorganisms and other biomass populations such as methanogens and sulfate-reducing bacteria.

11. Concentrations of the contaminant trans-DCE did not appear to decrease as a result of HRC application, which possibly reflects recalcitrance of this compound to biotransformation because of its chemical structure.

7.0 Recommendations

The following steps are recommended for future investigations of enhanced bioremediation at the STAR Center.

- Monitor concentrations of dissolved hydrogen for the following purposes:
  - quantifying total electron donor mass available to electron acceptors, particularly after the depletion of acetic acid
  - identifying temporal changes in TEAPs
  - identifying competition for hydrogen between dehalorespiring bacteria and other microorganisms such as sulfate reducers and methanogens

- Conduct microcosm tests for the following purposes:
  - identifying nutrient availability limitations in the surficial aquifer
  - identifying HRC longevity in aquifer materials
  - identifying and quantifying ancillary reactions between ferrous iron and other reduced constituents such as sulfide so that iron reduction processes are better quantified
  - identifying and quantifying Monod parameters for dechlorination of cis-DCE and VC
  - identifying factors that limit dechlorination of trans-DCE and mechanisms for promoting degradation of this contaminant

- Investigate the use of bioremediation amendments other than HRC with the intent of optimizing engineered dechlorination of DCE isomers and VC.

- Investigate ways for delivering bioremediation amendments such that
  - the deleterious effects of preferential flow in the surficial aquifer are minimized, and
  - the presence of the electron donors acetic acid and dissolved hydrogen is maintained for periods approaching several months to years

- Increase the number of monitoring wells used to gage the distribution of amendment transformation products and bioremediation performance in affected areas.

In the event that modeling is used in the future to simulate observations from microcosm or field tests, or to help design bioremedial actions, the following steps are recommended:

- Better define the stoichiometric relationships between all pertinent reactants, including all intermediate transformation products generated by the biotransformation of bioremediation amendments, and

- Simulate dissolved hydrogen as a separate reactant.

End of current text

8.0 References

Azadpour-Keeley, H.H. Russell, and G.W. Sewell, 1999. "Microbial Processes Affecting Monitored Natural Attenuation Contaminants in the Subsurface," U.S. Environmental Protection Agency, Ground Water Issue Paper, EPA/540/S-99/001.

Bradley, P.M., 2000. "Microbial Degradation of Chloroethenes in Groundwater Systems," *Hydrogeology Journal*, 8:104-111.

Bradley, P.M., and F.H. Chapelle, 1996. "Anaerobic Mineralization of Vinyl Chloride in Fe(III)-Reducing Conditions," *Environmental and Sciences Technology*, vol. 32, pp. 553-557.

Bradley, P.M., J.E. Landmeyer, and R.S. Dinicola, 1998. "Anaerobic Oxidation of [1,2^{-14}] Dichloroethene under Mn (IV)-Reducing Conditions." *Applied and Environmental Microbiology*, vol. 64, pp. 1560-1562.

Camp, Dresser, and McKee (CDM), 2003. *Bioavailable Ferric Iron Assay Report*, CDM Project Number 20944-36061-PINELLAS.

———, 1998. Microbial Mineralization of VC and DCE under Terminal Electron Accepting Conditions," *Anaerobe*, vol 4, pp. 81-87.

Chapelle, F.H., 2001. *Ground-Water Microbiology and Geochemistry*, John Wiley and Sons, Inc.

Chapelle, F.H., M.A. Widdowson, J.S. Brauner, E. Mendez III, and C.C. Casey, 2003. *Methodology for Estimating Times of Remediation Associated With Monitored Natural Attenuation*. U.S. Geological Survey, Water-Resources Investigations Report 03-4057.

Clement, T.P., 1998. *RT3D, A Modular Computer Code for Simulating Reactive Multi-species Transport in 3-Dimensional Groundwater Aquifers*, Pacific Northwest National Laboratory, PNNL-SA-1170.

Dolfing, J., 2000. "Energetics of Anaerobic Degradation Pathways of Chlorinated Aliphatic Compounds," *Microbial Ecology*, 40:2-7.

Domenico, P.A., and. F.W. Schwartz, 1990. *Physical and Chemical Hydrogeology*, John Wiley and Sons, Inc.

Essaid, H.I., B.A. Bekins, E. M. Godsy, E. Warren, M.J. Baedecker, and I.M. Cozarelli, 1995. "Simulation of Aerobic and Anaerobic Biodegradation Processes at a Crude Oil Spill Site," *Water Resources Research*, 31(12):3309-3327.

Essaid, H.I., and B.A. Bekins, 1997. "BIOMOC, A Multispecies Solute-Transport Model With Biodegradation," U.S. Geological Survey, Water-Resources Investigation Report 97-4022.

Fennel, D.E., J.M. Gossett, and S.H. Zinder, 1997. "Comparison of Butyric Acid, Ethanol, Lactic Acid, and Propionic Acid as Hydrogen Donors for the Reductive Dechlorination of Tetrachloroethene," *Environmental Science and Technology*, 31:918-926.

Fournier, L.B., 2003. "Aerobic, Co-Metabolic In Situ Biodegradation of Chlorinated Solvents and Horizontal Biosparge Wells – A Match Made in Bioremediation Heaven," *Ground Water*, 41(6):727-728.

Freeze, R.A., and J.A. Cherry, 1979. *Groundwater*, Prentice-Hall Inc., Englewood Cliffs, New Jersey.

Gelhar, L.W., A. Mantoglou, C. Welty, and K.R. Rehfeldt, 1985. "A Review of Field-Scale Physical Solute Transport Processes in Saturated and Unsaturated Porous Media, Electric Power Research Institute," EA-4190, Research Project 2485-5.

He, J., Y. Sung, M.E. Dollhopf, B.A. Fathepure, and F.E. Loffler, 2002. "Acetate Versus Hydrogen as Direct Electron Donors to Stimulate the Microbial Reductive Dechlorination Process at Chloroethene-Contaminated Sites," *Environmental Science and Technology*, 36:3945-3952.

Heron, G., C. Crouzel, A.C.M. Bourg, and T.H. Christensen, 1994. "Speciation of Fe (II) and Fe (III) in Contaminated Aquifer Sediments Using Chemical Extraction Techniques," *Environmental Science and Technology*, 26:1698-1705.

Kennedy, L., J. Everett, and J. Gonzales, undated. *Aqueous and Mineral Intrinsic Bioremediation Assessment (AMIBA) Protocol*, U.S. Air Force Center for Environmental Excellence.

Kennedy, L.G., J.W. Everett, K.J. Ware, R. Parsons, and V. Green, 1998. "Iron and Sulfur Mineral Analysis Methods for Natural Attenuation Assessments," *Bioremediation Journal*, 3:259-275.

Kindred, J.S., and M.A. Celia, 1989. "Contaminant Transport and Biodegradation, 2. Conceptual Model and Test Simulations," *Water Resources Research*, 25(6):1149-1159.

Konikow, L.F., and J.D. Bredehoeft, 1978. *Computer Model of Two-Dimensional Solute Transport and Dispersion in Ground Water*, S.S. Geological Survey, Techniques of Water-Resources Investigations, Book 7 Chapter C2.

Major, D., E. Endwards, P. McCarty, J. Gossett, E. Hendrickson, F. Loeffler, S. Zinder, D. Ellis, J. Vidumsky, M. Harkness, G. Klecka, and E. Cox, 2003. "Discussion of Environment vs. Bacteria or Let's Play 'Name That Bacteria," *Ground Water Monitoring and Remediation*, 23(2):32-48.

McCarty, P.L., 1997. "Breathing with Chlorinated Solvents," *Science*, 276:1521-1522.

McCullough, J., T.C. Hazen, S.M. Benson, F. B. Metting, and A.C. Palmisano, 1999. *Bioremediation of Metals and Radionuclides…What it is and How it Works, a NABIR Primer*, U.S. Department of Energy, Natural and Accelerated Bioremediation Research (NABIR) Program, LBNL-42595, 58 p.

Monod, J., 1949. "The Growth of Bacterial Cultures," *Annual Review of Microbiology*, 3:371−394.

National Research Council (NRC), 2000. *Natural Attenuation for Groundwater Remediation*, National Academy Press, Washington, D.C., 274 p.

Regenesis, 2003a. *Biological Reductive Dechlorination of CAHs*, HRC Technical Bulletin 1.1.2.

———, 2003b. *Using Organic Substrates to Promote Biological Reductive Dechlorination of CAHs*, HRC Technical Bulletin 1.1.3.

———, 2003c. C*ompetition for Hydrogen Between Reductive Dechlorinators and Other Microorganisms*, HRC Technical Bulletin 1.1.4.

Regenesis, 2003d. *Distribution of HRC in the Aquifer*, HRC Technical Bulletin 2.8.2.

———, 2003e. Hydrogen Release Compound (HRC).

Safety and Ecology Corporation (SEC), 2003a. *Remediation Plan for In-Situ Enhanced Bioremediation Technology to Control the Plume of Dissolved Contaminants at the Building 100 Area of the Young-Rainey STAR Center Pilot Test.*

Safety and Ecology Corporation (SEC), 2003b. *Injection Completion Report*, April.

Skeen, R.S., J. Gao, B.S. Hooker, and R.D. Quesenberry, 1996. *Characterization of Anaerobic Chloroethene-Dehalogenating Activity in Several Subsurface Sediments*, Pacific Northwest National Laboratory, PNNL-11417.

Smatlak, C.R., J.M. Gossett, and S.H. Zinder, 1996. "Comparative Kinetics of Hydrogen Utilization for Reductive Dechlorination of Tetrachloroethene and Methanogenesis in an Anaerobic Enrichment Culture," *Environmental Science and Technology*, 30:2850-2858.

Tiedje, J.M., and F.E. Loffler, 1999. *Complete Detoxification of Short Chain Chlorinated Aliphatic Compounds: Isolation of Halorespiring Organisms and Biochemical Studies of the Dehalogenating Enzyme Systems*, final report to the U.S. Department of Energy, Grant Number DE_FG07-96ER62319, Project Number 55105, 23 p.

Tuccillo, M.E., I. Cozzarelli, and J.S. Herman, 1999. "Iron Reduction in the Sediments of a Hydrocarbon-Contaminated Aquifer," *Applied Geochemistry*, 14:655-667.

U.S. Department of Energy (DOE), 1998. "Cost and Performance Report, In Situ Anaerobic Bioremediation, Pinellas Northeast Site, Largo Florida," Innovative Treatment Remediation Demonstration, April.

———, 2003a. *Pinellas Environmental Restoration Project Performance Evaluation for the Biosparging System at the 4.5 Acre Site at the Young - Rainey STAR Center*, GJO-2003-426-TAC, April.

———, 2003b. *Simulation of Enhanced Bioremediation at the Building 100 Area*, GJO-2003-495-TAC, PIN 700.20.10.

Vroblesky, D.A., and F.H. Chapelle, 1994. “Temporal and Spatial Changes of Terminal Electron-Accepting Processes in a Petroleum-Contaminated Aquifer and the Significance for Contaminant Biodegradation,” *Water Resources Research*, 30(5):1561-1570.

Watson, I.A., S.E. Oswald, K.U. Mayer, Y.Wu, and S.A. Banwart, 2003. “Modeling Kinetic Processes Controlling Hydrogen and Acetate Concentrations in an Aquifer-Derived Microcosm,” *Environmental Science and Technology*, 37:3910-3919.

Xpert Design and Diagnostics, LLC, 2003. *Biosparging Performance Review Report*, Pinellas 4.5 Acre Site, Florida.

Yang, Y, and P.L. McCarty, 1998. “Competition for Hydrogen Within a Chlorinated Solvent Dehalogenating Anaerobic Mixed Culture”, *Environmental and Sciences Technology*, vol. 32, pp. 3591-3597.

Figures

This page intentionally left blank

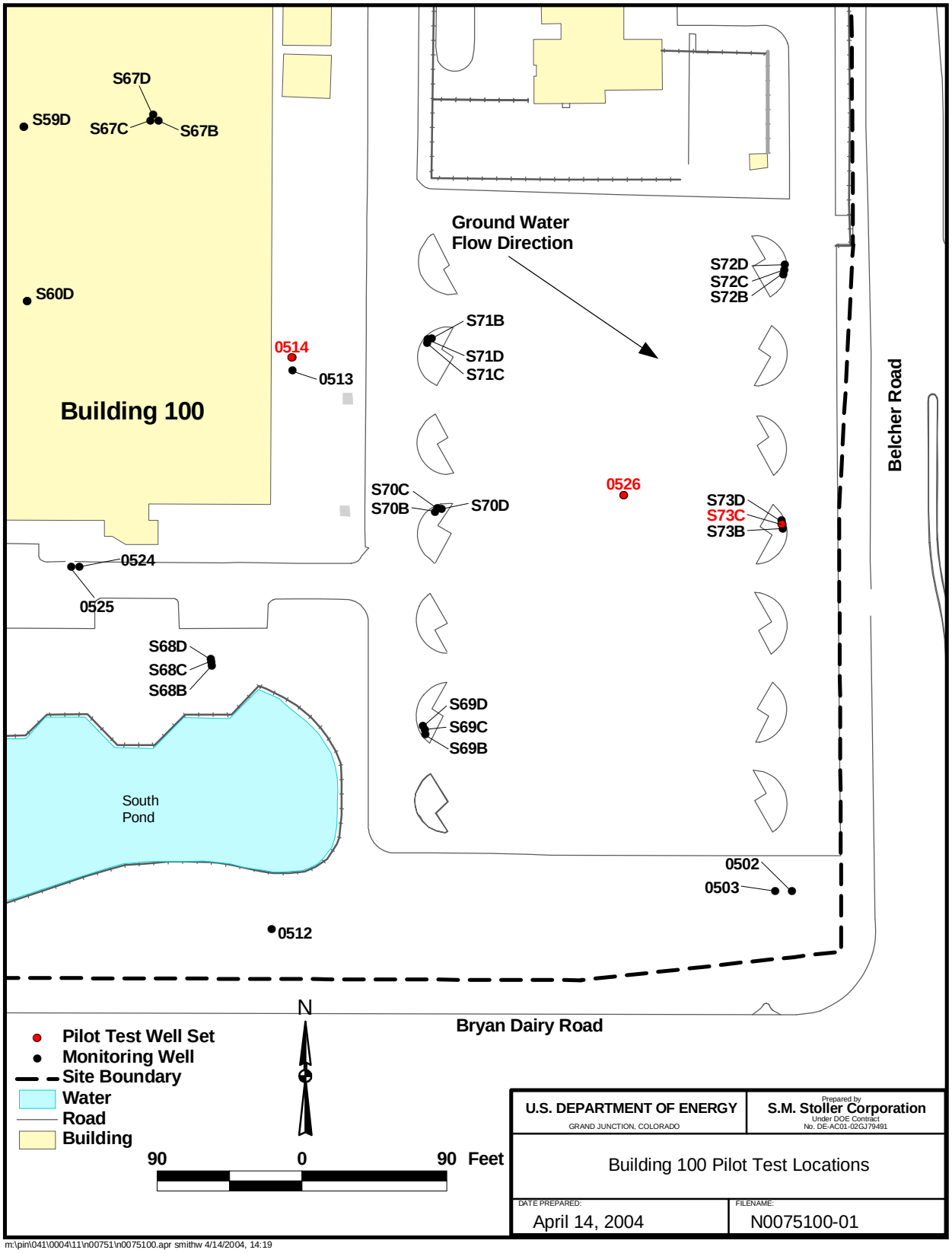

Figure 1. Building 100 Pilot Test Areas

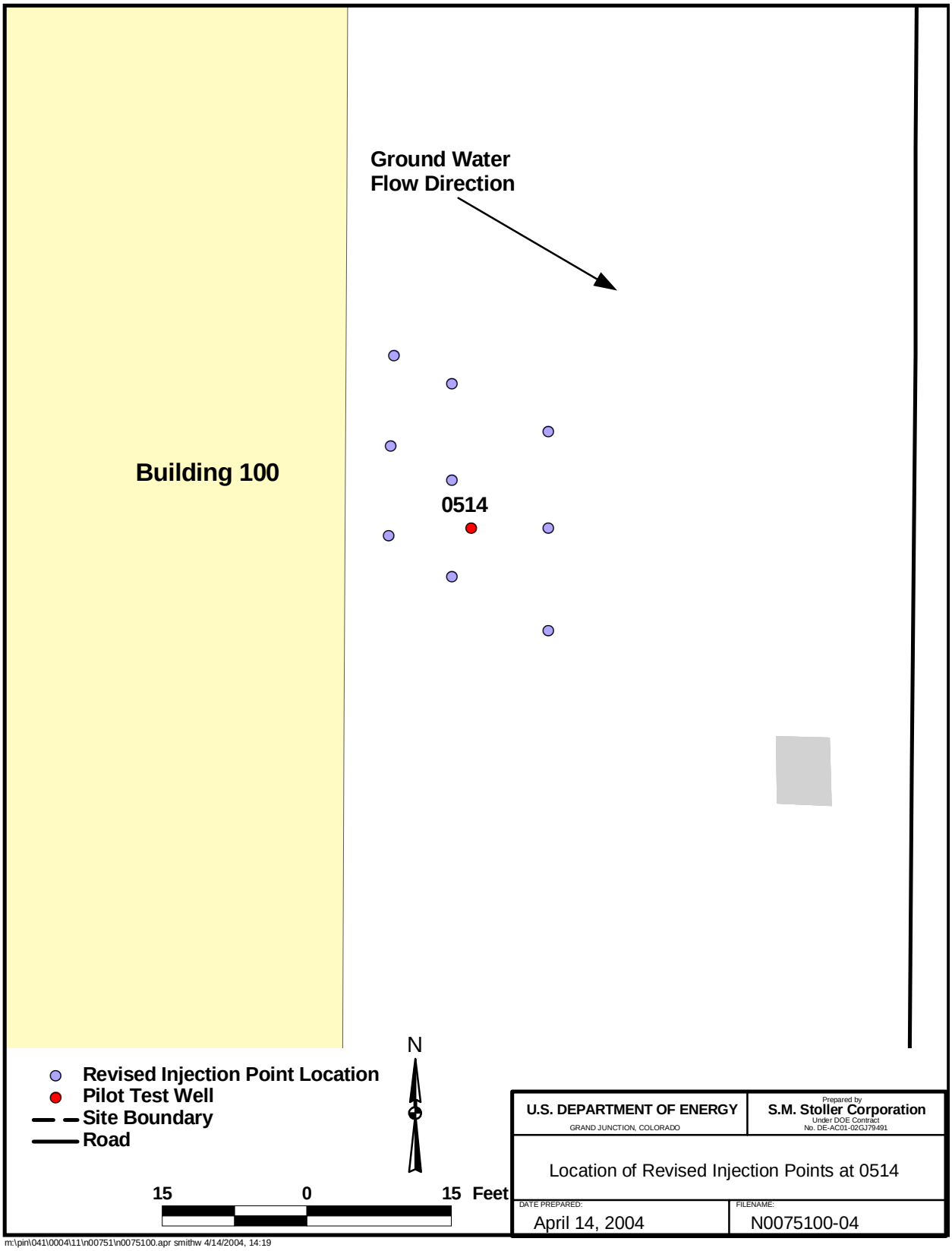

Figure 2. Injection and Monitoring Location at Pilot Test Area 0514

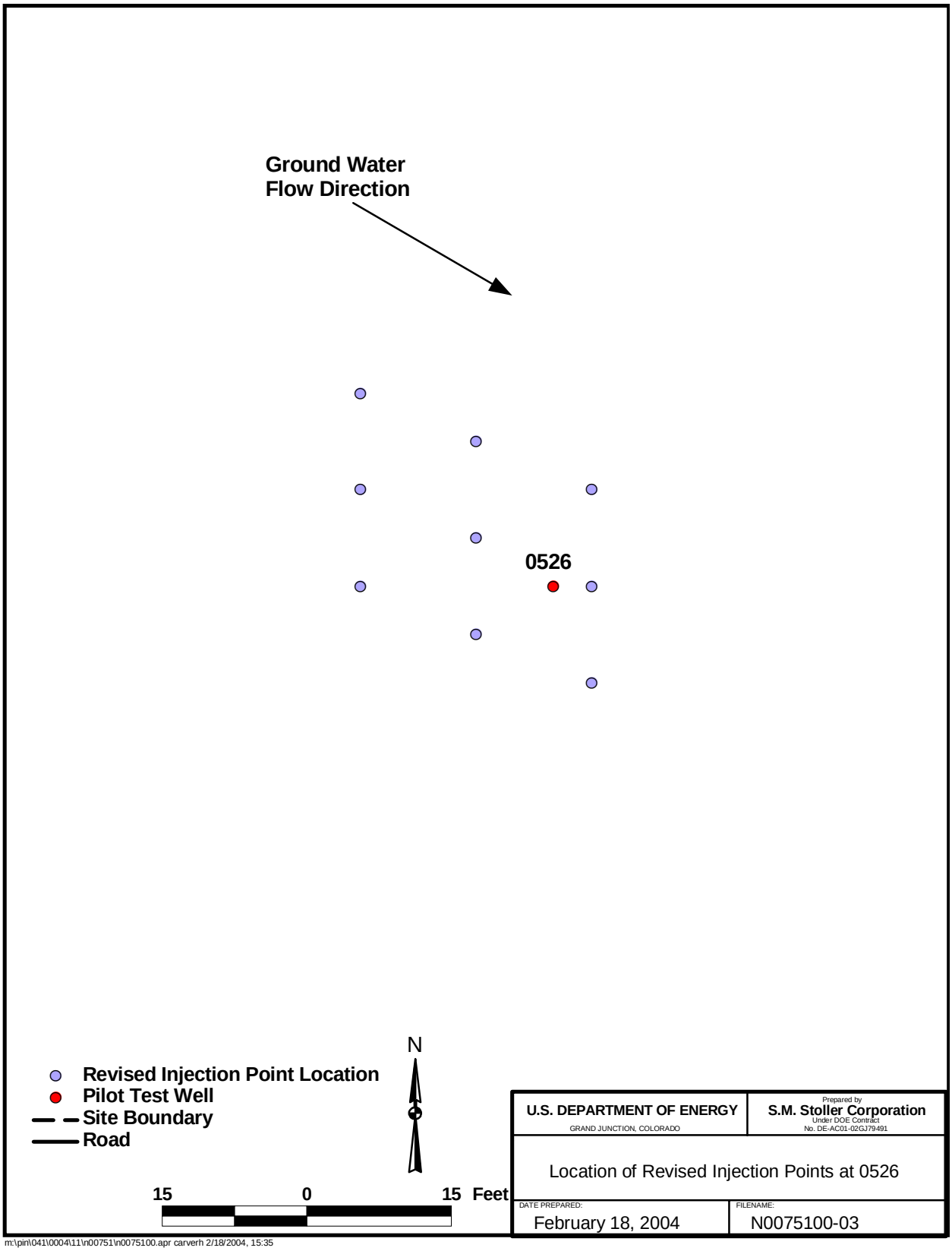

Figure 3. Injection and Monitoring Locations at Pilot Test Area 0526

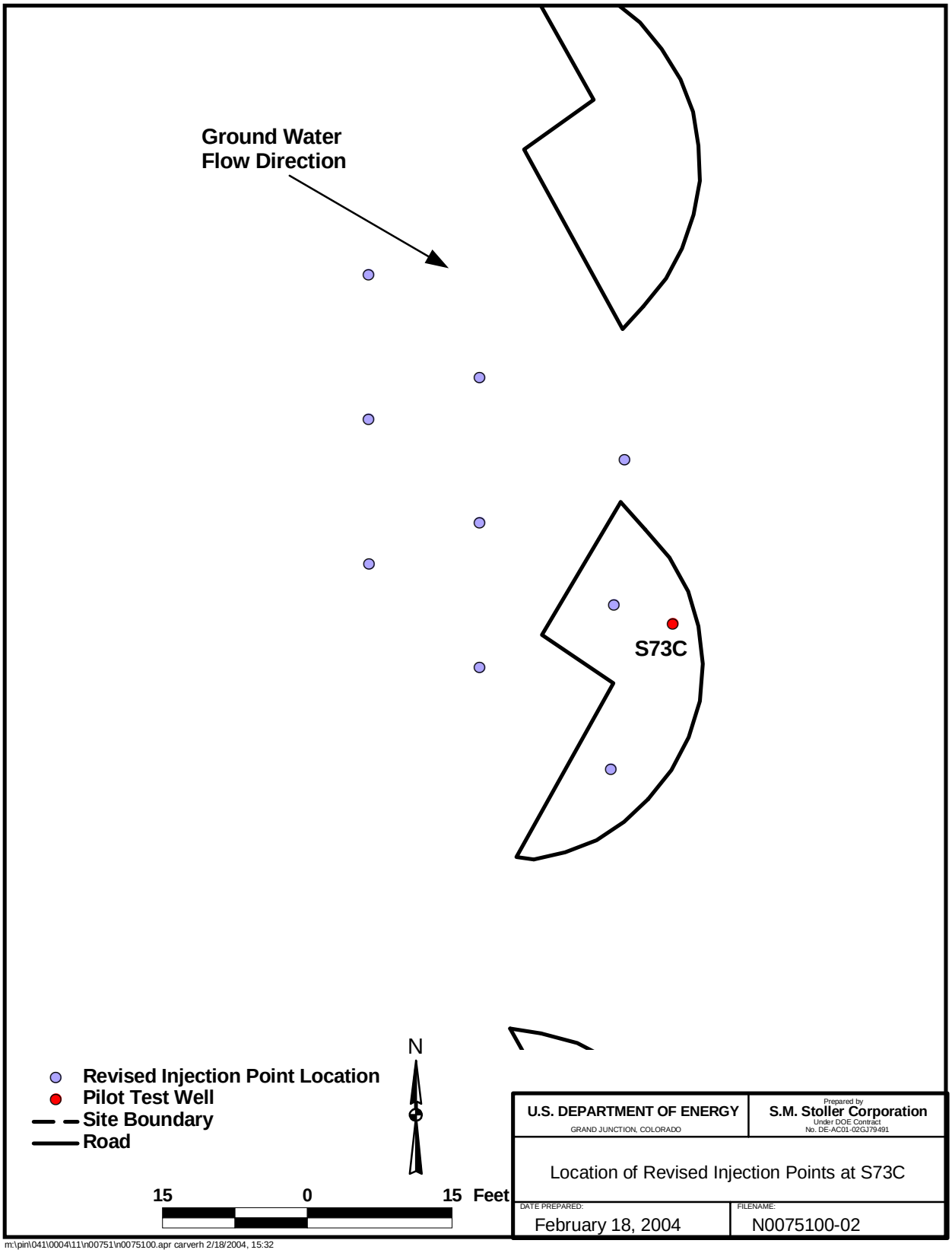

Figure 4. Injection and Monitoring Locations at Pilot Test Area S73C

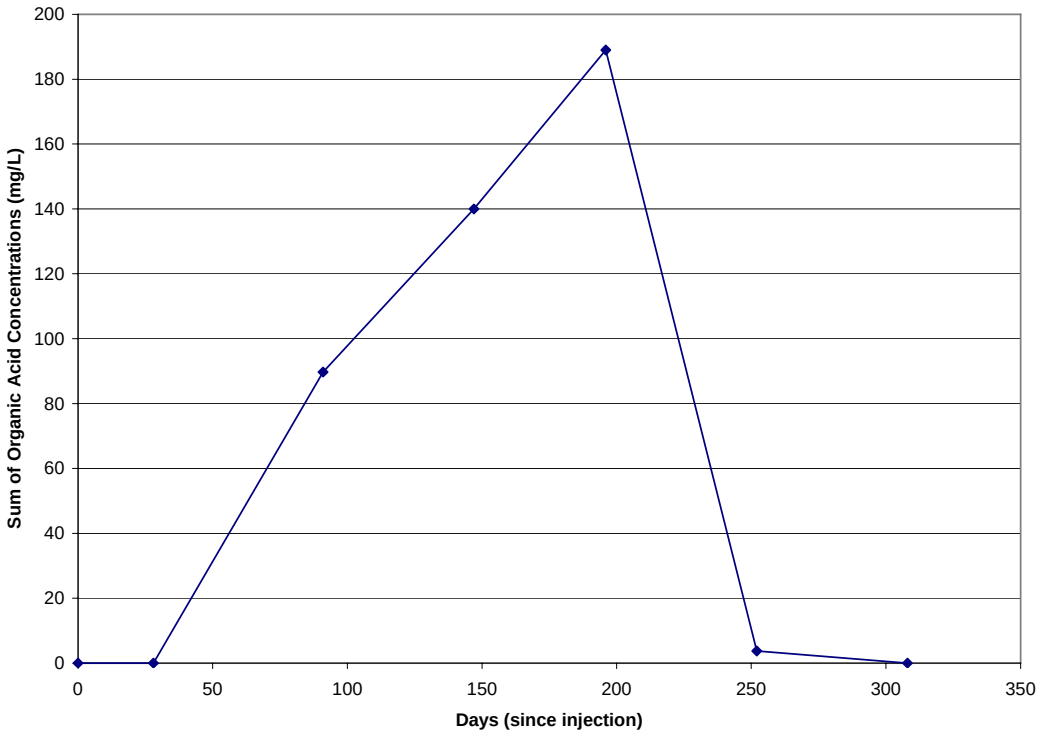

Figure 5. Sum of Organic Acid Concentrations Observed at Well 0514 During the Bioremediation Pilot Test

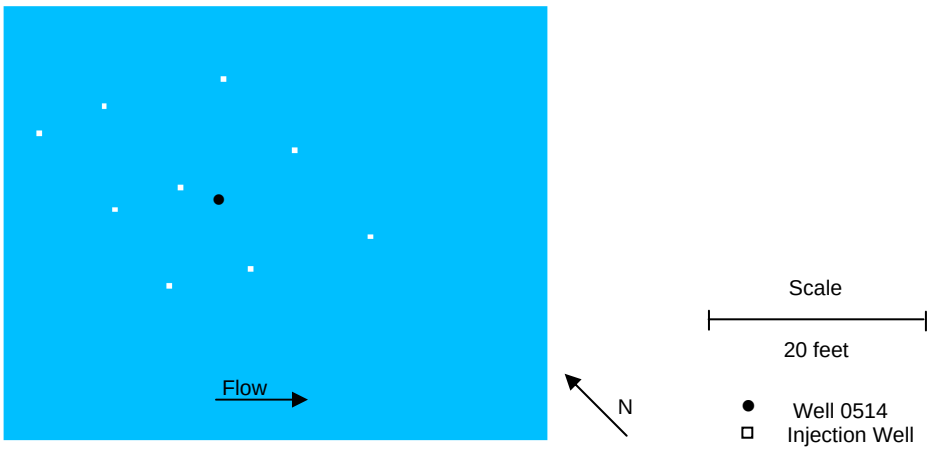

Figure 6. Simulation Area Near Monitor Well 0514

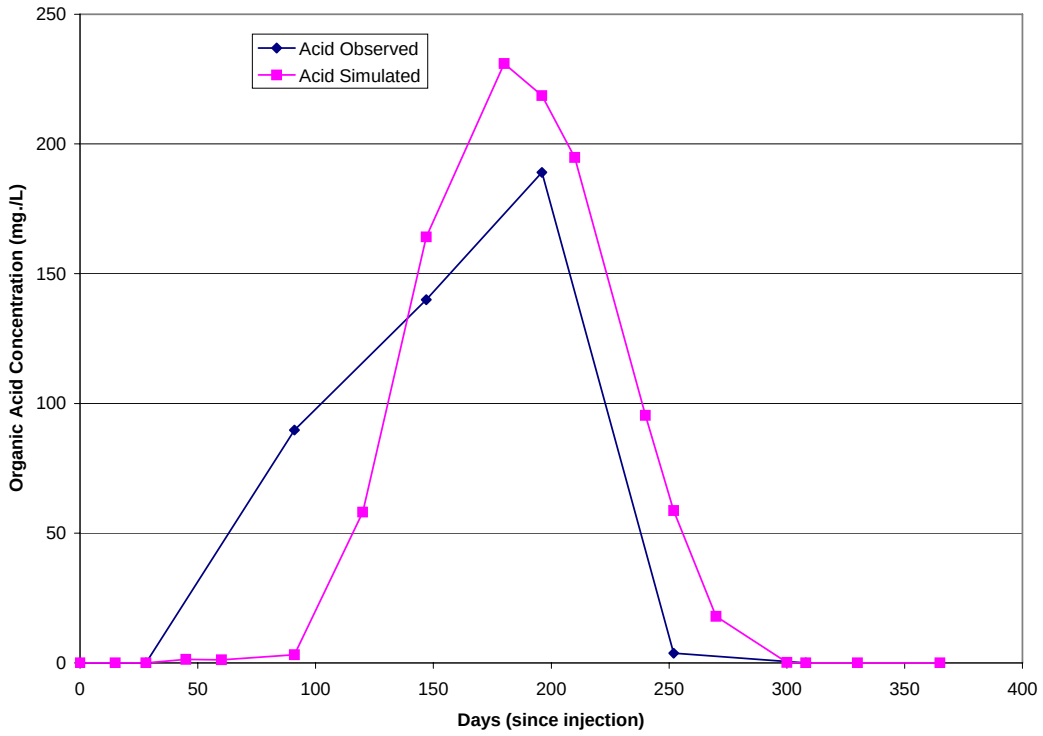

Figure 7. Total Organic Acid Concentrations at Monitoring Well 0514 During the Pilot Test

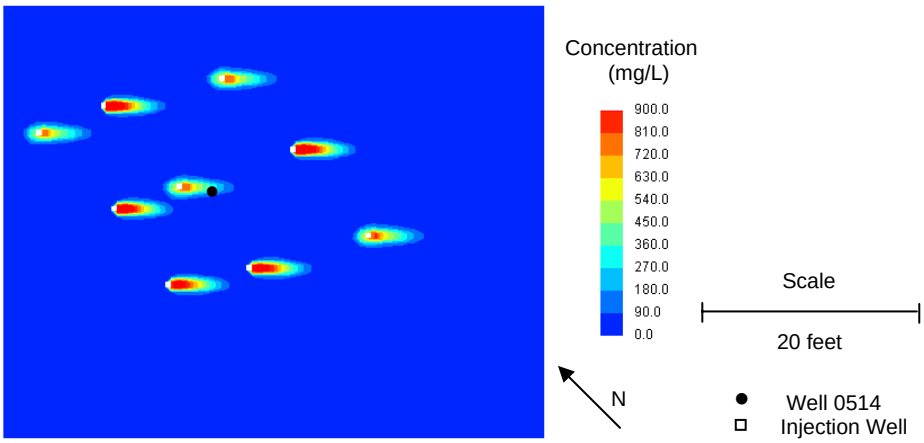

Figure 8. Simulated Organic Acid Concentrations (mg/L) Two Months After HRC Injection

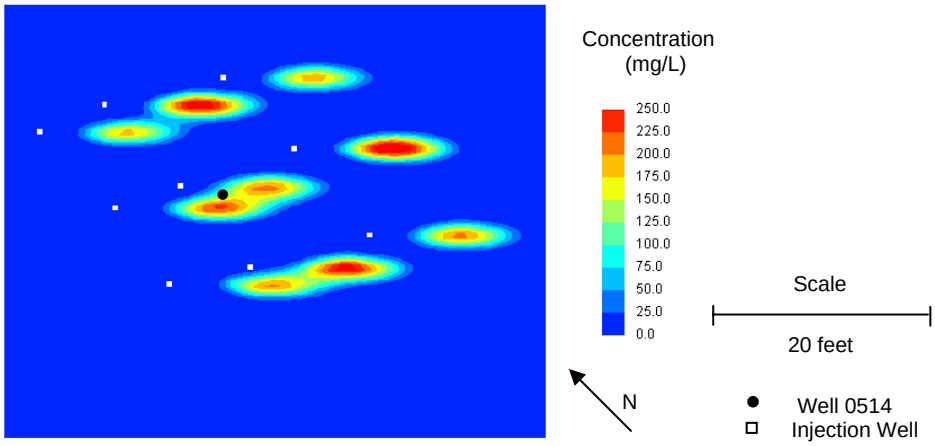

Figure 9. Simulated Organic Acid Concentrations (mg/L) 6.5 Months After HRC Injection

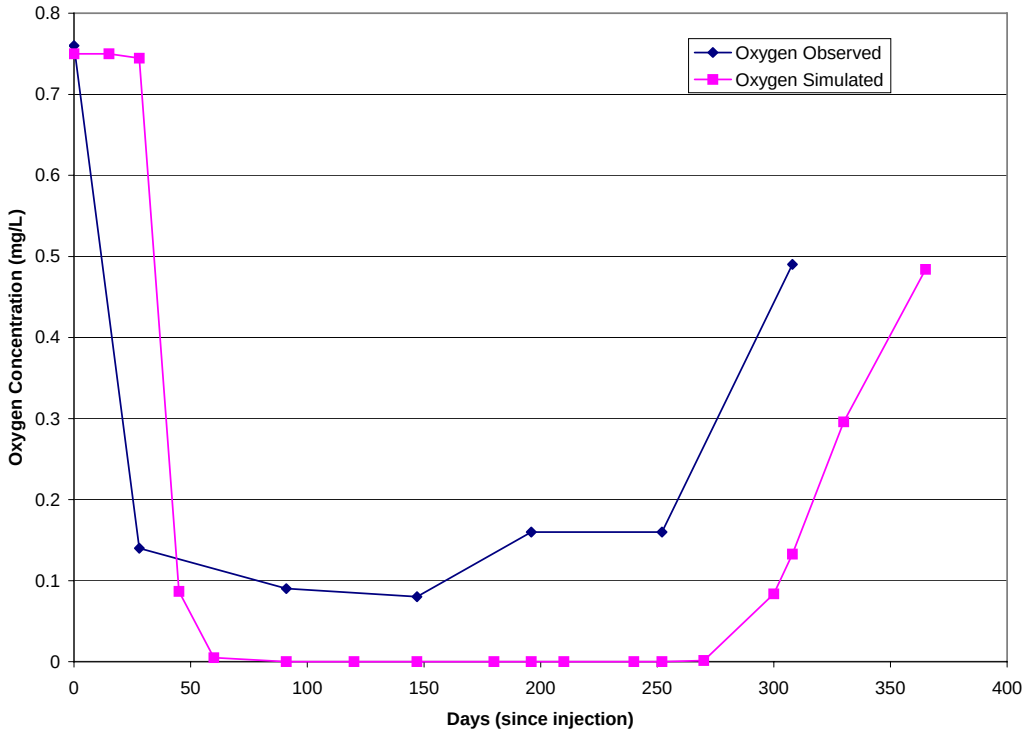

Figure 10. Dissolved Oxygen Concentrations at Monitor Well 0514 During the Pilot Test

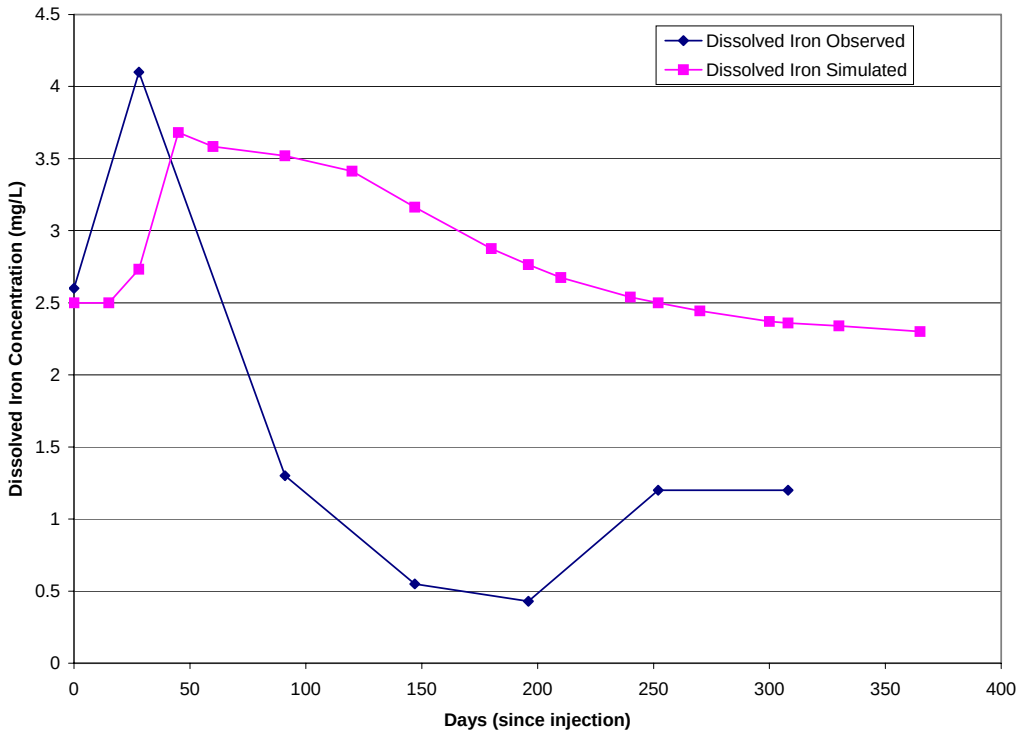

Figure 11. Dissolved Iron Concentrations at Monitor Well 0514 During the Pilot Test

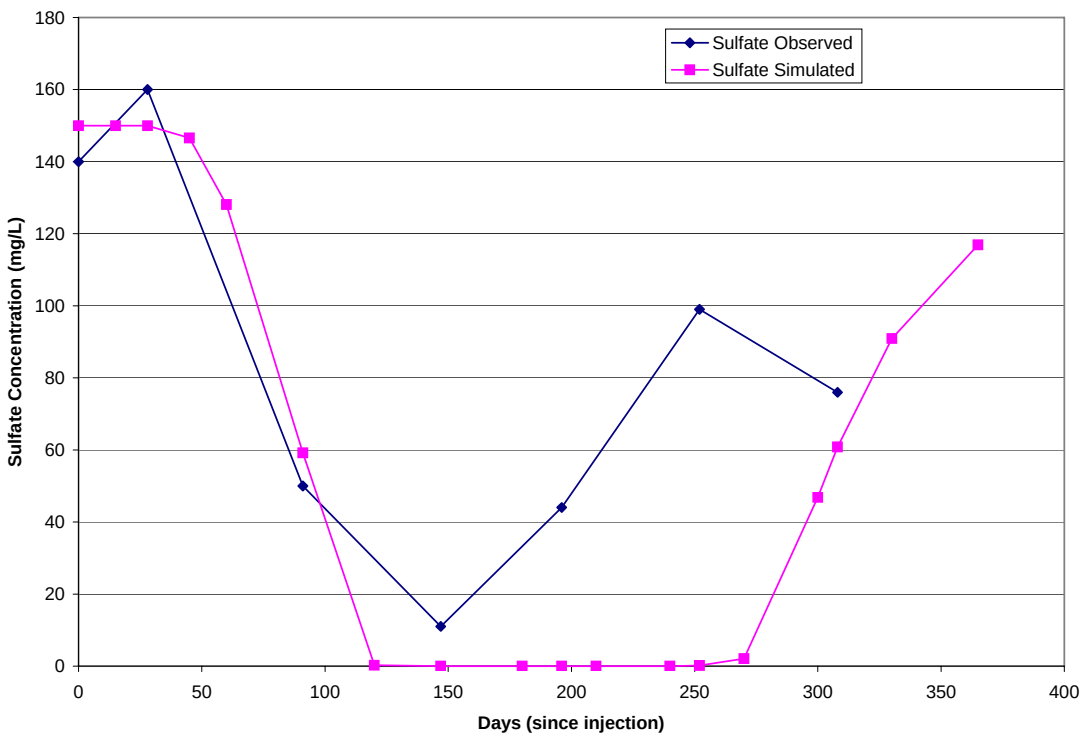

Figure 12. Dissolved Sulfate Concentrations at Monitor Well 0514 During the Pilot Test

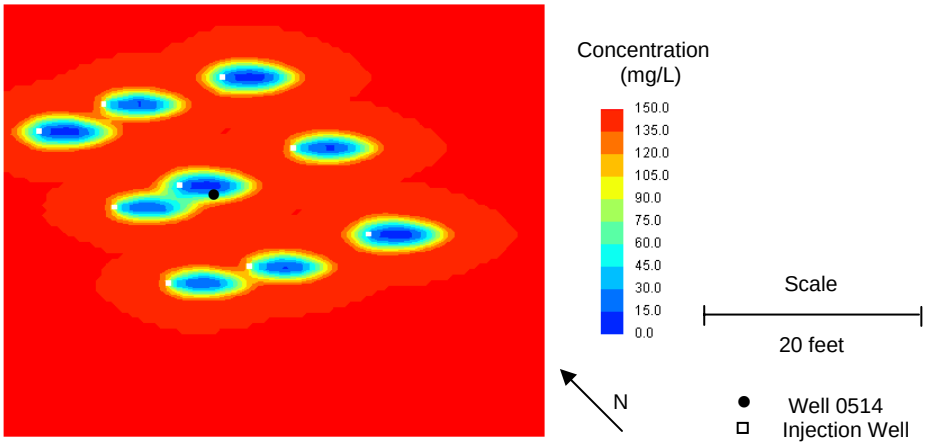

Figure 13. Simulated Sulfate Concentrations (mg/L) Two Months After HRC Injection

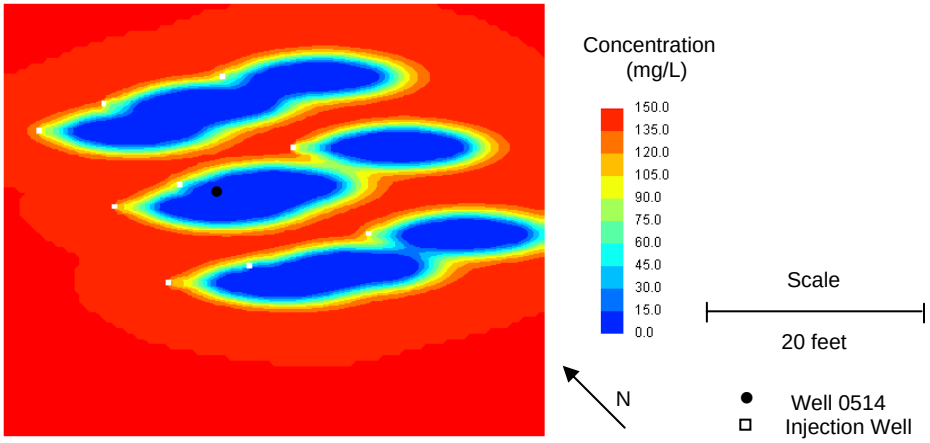

Figure 14. Simulated Sulfate Concentrations (mg/L) 6.5 Months After HRC Injection

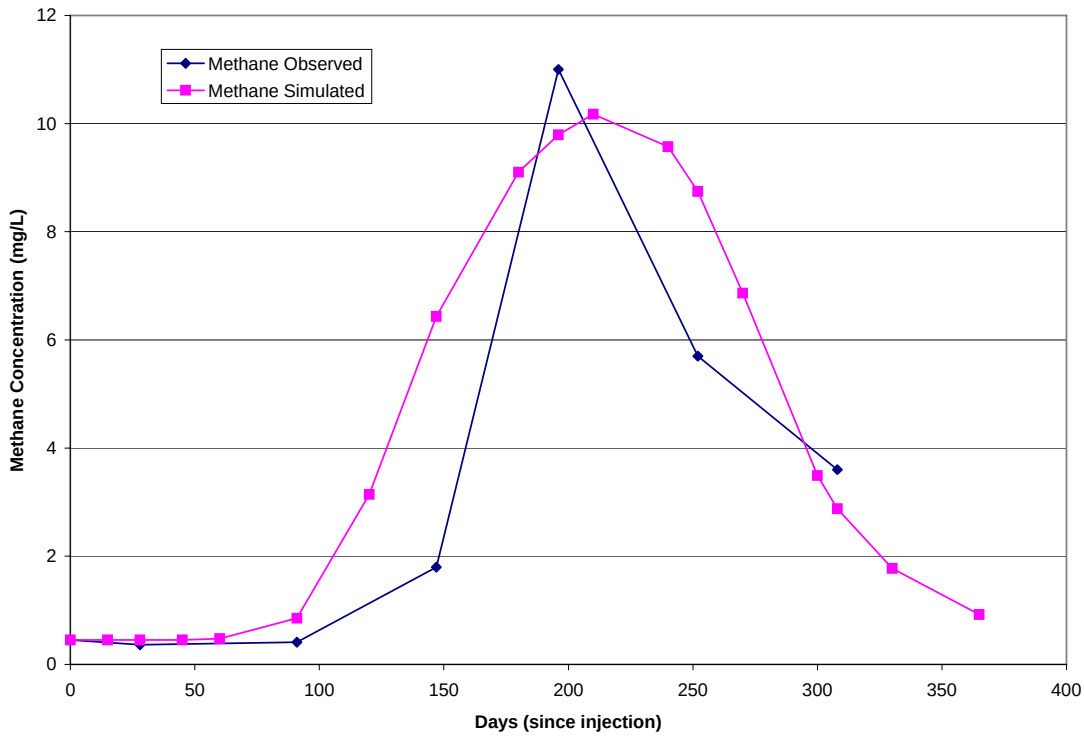

Figure 15. Dissolved Methane Concentrations at Monitor Well 0514 During the Pilot Test

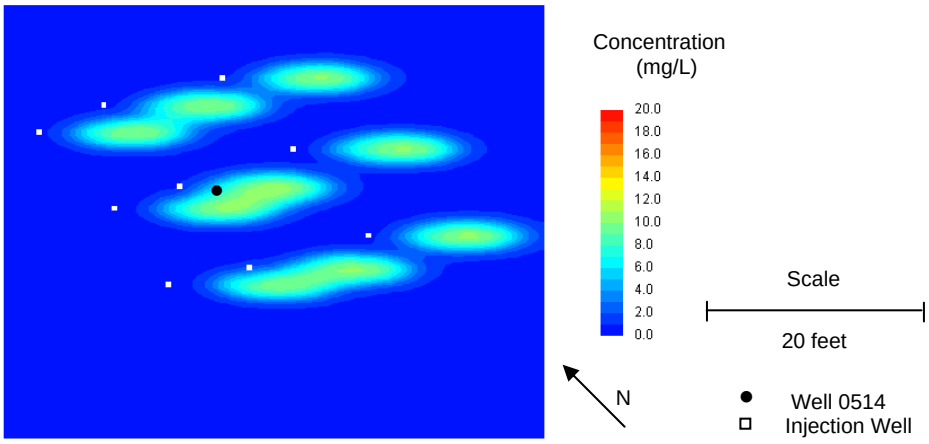

Figure 16. Simulated Methane Concentrations (mg/L) 6.5 Months After HRC Injection

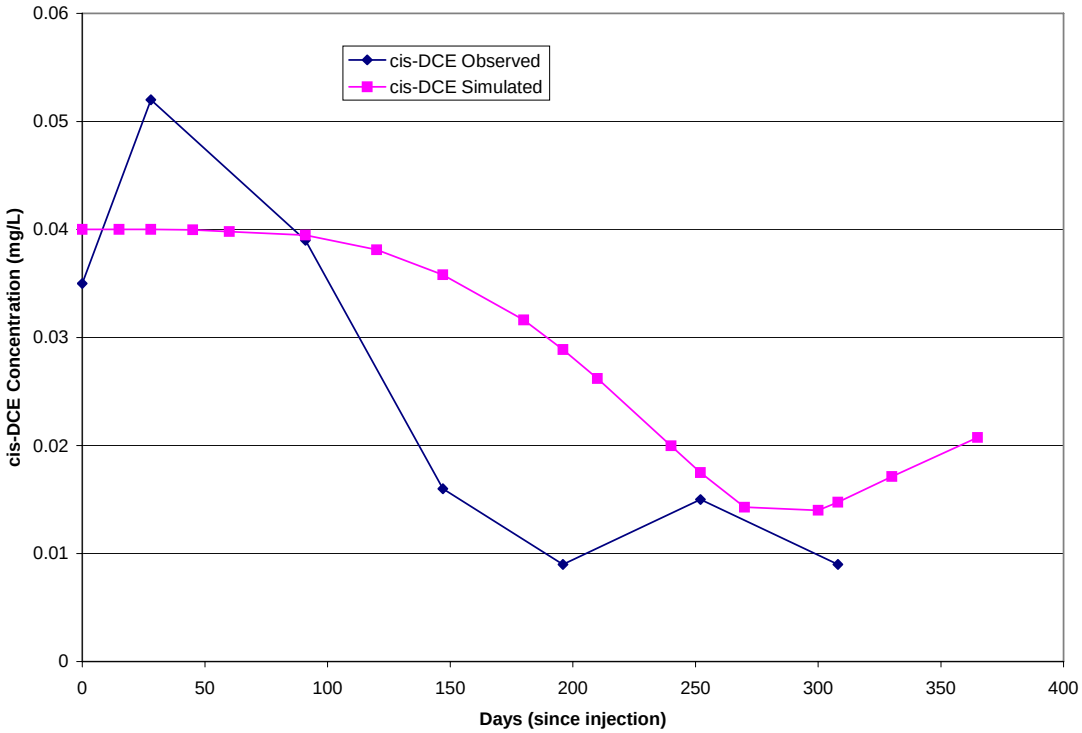

Figure 17. Dissolved cis-DCE Concentrations at Monitor Well 0514 During the Pilot Test

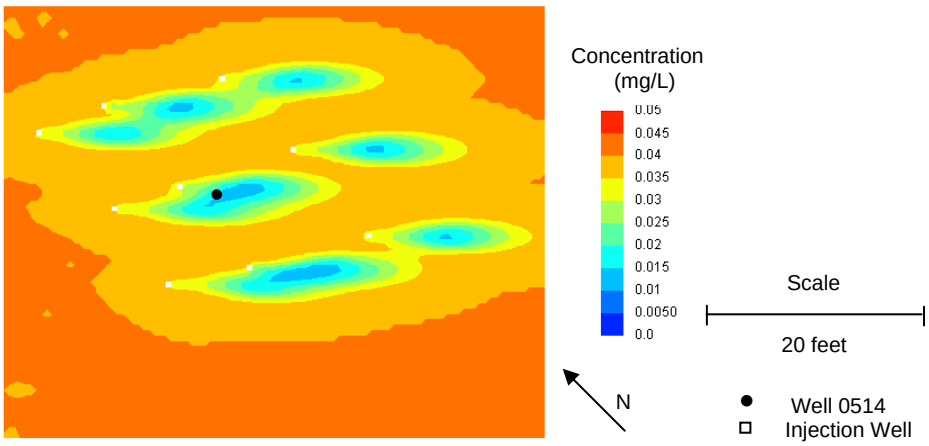

Figure 18. Simulated cis-DCE Concentrations (mg/L) Nine Months After HRC Injection

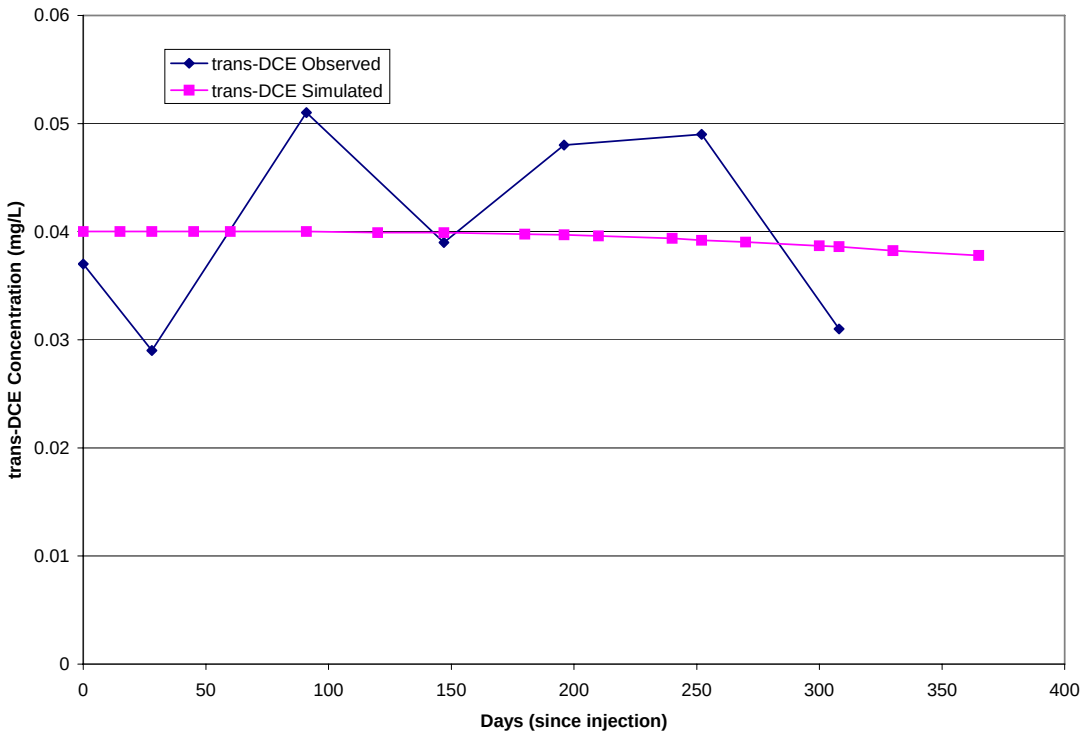

Figure 19. Dissolved trans-DCE Concentrations at Monitor Well 0514 During the Pilot Test

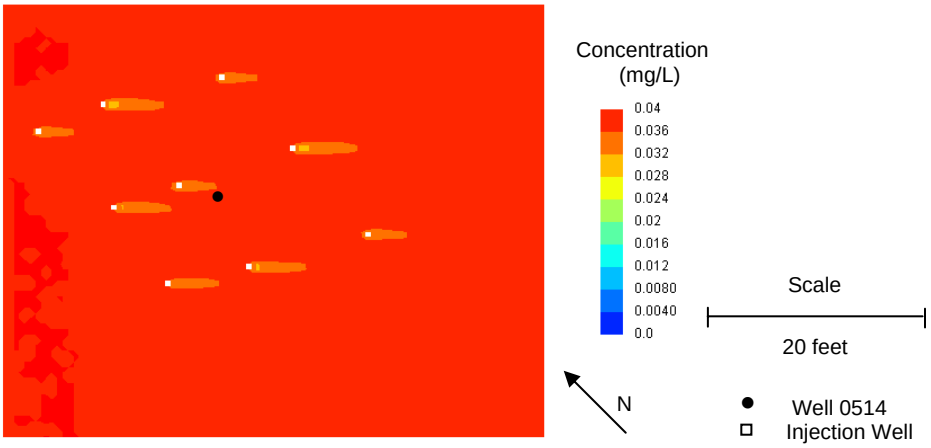

Figure 20. Simulated trans-DCE Concentrations (mg/L) Nine Months After HRC Injection

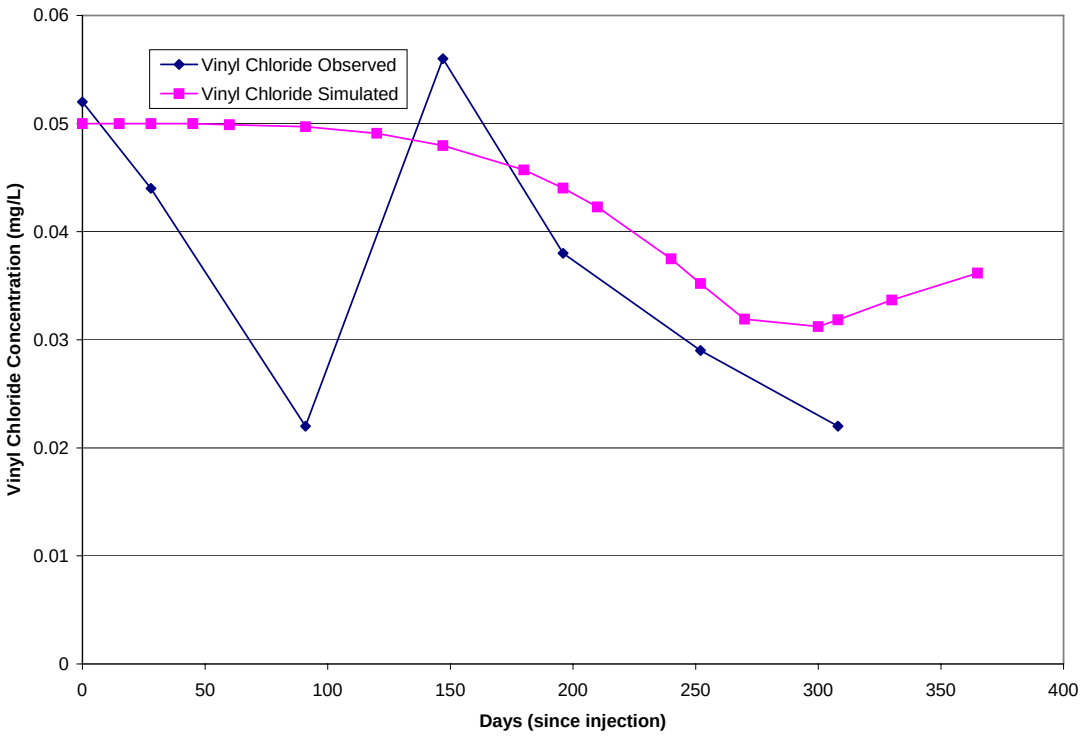

Figure 21. Dissolved Vinyl Chloride Concentrations at Monitor Well 0514 During the Pilot Test

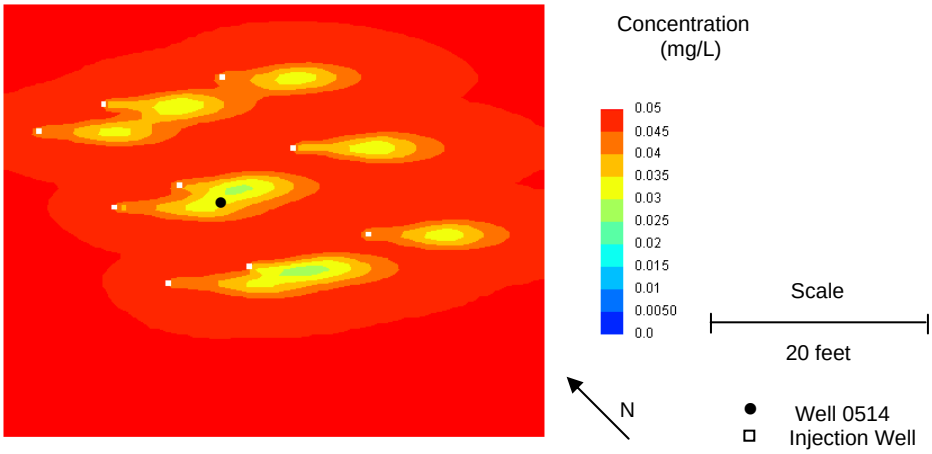

Figure 22. Simulated Vinyl Chloride Concentrations (mg/L) Nine Months After HRC Injection

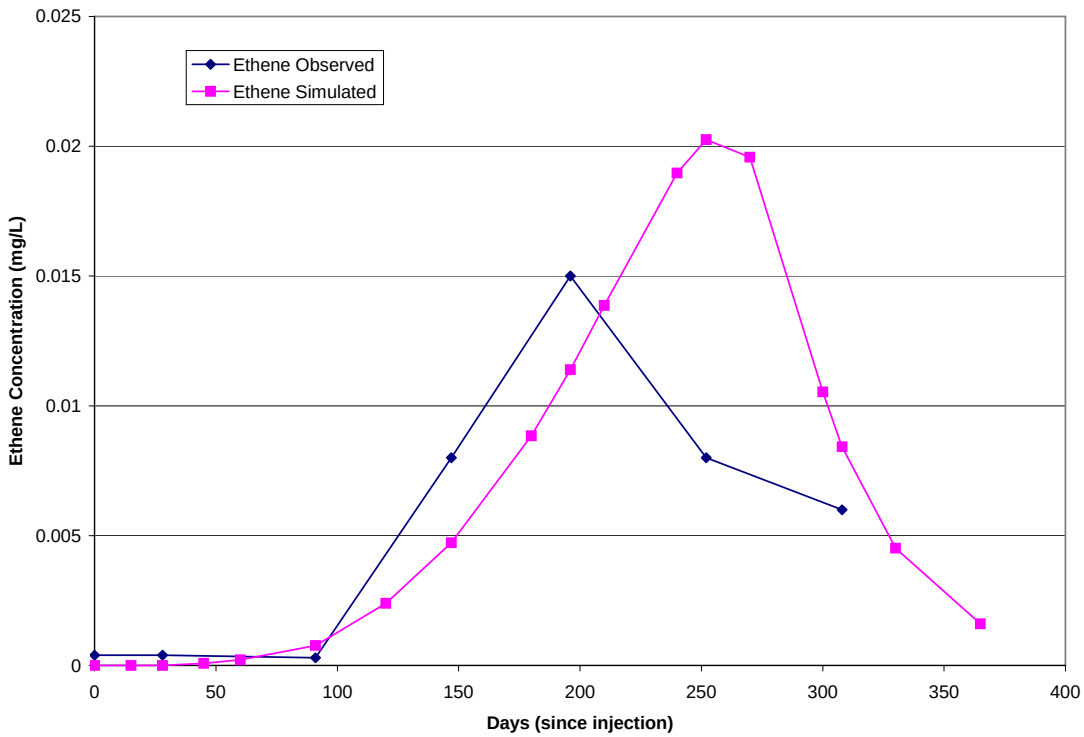

Figure 23. Dissolved Ethene Concentrations at Monitor Well 0514 During the Pilot Test

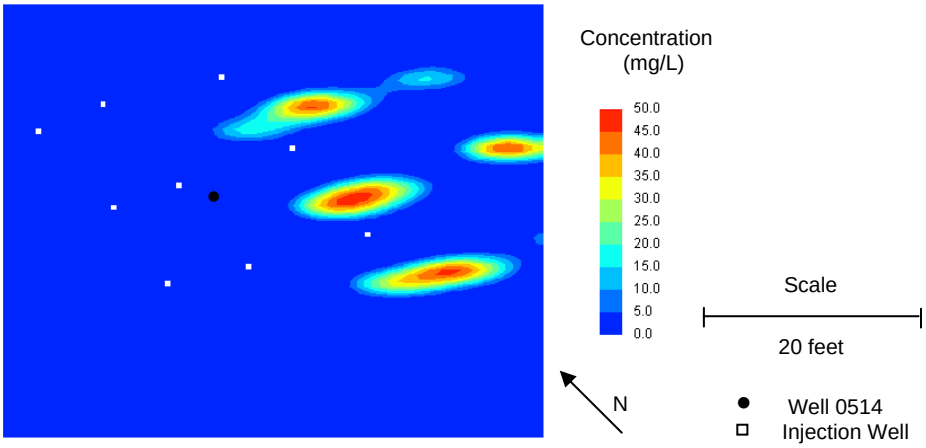

Figure 24. Predicted Organic Acid Concentrations (mg/L) One Year After HRC Injection

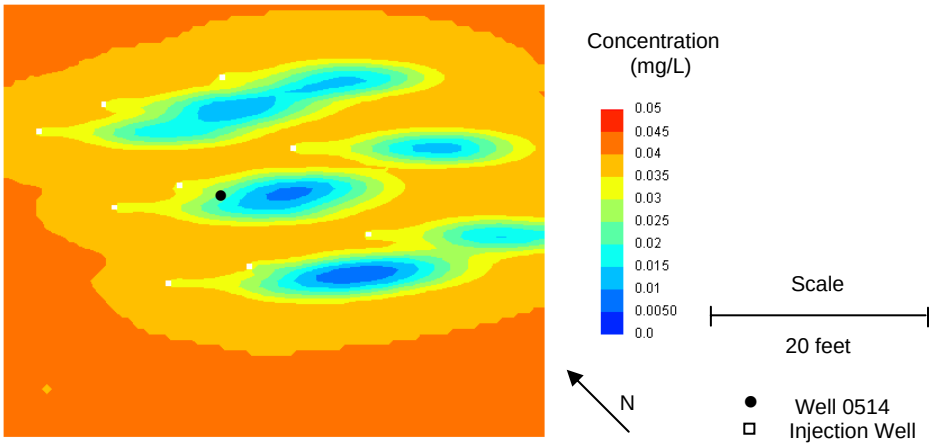

Figure 25. Predicted cis-DCE Concentrations (mg/L) One Year After HRC Injection

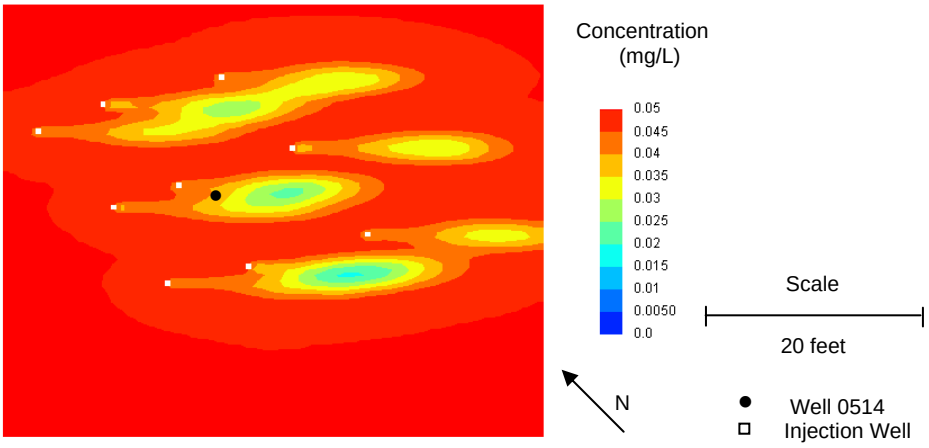

Figure 26. Predicted Vinyl Chloride Concentrations (mg/L) One Year After HRC Injection

End of current text